TEL AVIV UNIVERSITY
RAYMOND AND BEVERLY SACKLER
FACULTY OF EXACT SCIENCES
SCHOOL OF PHYSICS & ASTRONOMY

אוניברסיטת תל-אביב
הפקולטה למדעים מדוייקים
ע"ש ריימונד ובברלי סאקלר
בית הספר לפיסיקה ואסטרונומיה

Two-Dimensional Polymers with Random Coulomb Interactions

by

Eilon Brenner

Thesis submitted in partial
fulfillment of the requirements
for the M.Sc. degree
at Tel-Aviv University
School of Physics and Astronomy

The research work for this thesis has been
carried out under the supervision of
Professor Yacov Kantor

June 1997

Acknowledgments

I would like to thank my supervisor, Professor Yacov Kantor, for his guidance. His knowledge and experience were crucial to make this work possible.

I have benefited greatly from the collaboration and support of my fellow student Ido Golding. I would also like to thank my colleagues Oded Farago, Itamar Borukhov and Haim Diamant for their assistance and good company while this work was carried out.

I owe special gratitude to my family for their encouragement and moral support.

Contents

Abstract

We study the properties of a polymer on a 2-dimensional lattice whose monomers are charges interacting through a long-range, logarithmic, Coulomb potential (2-dimensional *polyampholyte*). We investigate energetic and configurational properties of the system under variations of temperature and charge distribution along the polymer. Different ensembles of quenched and annealed disorder are studied and compared.

Results are obtained by enumerating all possible configurations of a specific chain and calculating exact thermodynamic variables. We study complete ensembles of all possible charge sequences up to a length of 18 monomers. Partial ensembles of lengths up to 26 monomers were also enumerated. The results are compared to analytic estimations of the expected behavior.

We study the properties of the ground states of the ensemble. The ground state energy of the neutral ensemble is shown to be extensive and self-averaging. We find the dependence of the energy spectrum and the typical size on the excess charge of the polymer. Only the strictly neutral ensemble collapses to a compact configuration. This effect is much more pronounced when we observe the ground state properties of the annealed ensemble. For a minimal excess charge it expands to a fully extended configuration.

The crossover from the high-temperature to low-temperature behavior is investigated. The first deviation of the average configuration from random behavior at high temperatures to a compact or extended typical size is determined by a critical excess charge that increases with the length of the polymer.

Specific quenches are shown to possess interesting properties, different than the average behavior. A sequence of alternating-sign charges probably undergoes a Θ-transition, similar to short-range interacting systems. The homogeneously charged polymer will remain in its fully extended ground state at all finite temperatures.

We also search for indications of a possible low-temperature freezing transition and a glass-like energy landscape. We apply different criteria to the study of this question. It seems that the system does not exhibit this phenomenon.

The behavior of our model is very much affected by the properties of the Coulomb interaction in two dimensions. We devote some attention to the discussion of its features and derive some general results concerning the energy of a system of two dimensional charges.

1 Introduction

1.1 Polymers

A polymer is a structure of connected units called monomers, usually of a limited variety. Polymers of interest usually consist of many such units, forming a relatively flexible macromolecule that has many interesting properties on a macroscopic scale. In real polymers the monomers are connected by covalent bonds, whose energy is much larger than the typical k_BT, and can, therefore, be assumed to be unbreakable. The simplest case, we discuss here, is a linear polymer chain in which N monomers are connected one to another in a linear sequence.

Polymer systems have been subject to extensive study for several decades ([1, 2, 3]). The interest in such macromolecules arises from several sources: the most commonly quoted, is their natural occurrence in biological systems, for example proteins. Artificial polymers are very common in everyday life and are of great commercial and industrial value. From the theoretical point of view, different random polymer models share many common features with many physical systems exhibiting randomness or frustration (such as spin glasses) that have been subject to extensive physical research [4].

Polymers may be classified by the type of building blocks from which they are composed. The simplest case would be that all the monomers are identical. These are called *homopolymers*. Polymers in which there are several types of monomers are known as *heteropolymers* or *copolymers*. Biopolymers such as proteins and DNA are members of this class. If the molecule contains charged links then it is known as a *polyelectrolyte*. Usually, the neutrality of the system demands the opposite charge to be in the solvent, or at some distant "charge bath". However, there are cases when the chain itself will carry both types of opposite charges. These are known as *polyampholytes* [5] (PA henceforth), and they are the subject of the present discussion.

In real polymers there are many types of interactions between the monomers. At short distances, most of them will be more dominant than the Coulomb interaction. However, all these die out very quickly and at length scales on the order of magnitude of a real polymer's size, only the Coulomb interaction prevails, if it is not screened (usually it is). For this reason we devote our study to it, its effect on the energy spectrum and its governing the spatial arrangement of the polymer.

It is common to consider complex systems of polymers: a single polymer restricted

to a finite volume, several co-existing polymers, a system where polymers may connect with others forming networks or gels and up to the more complex arrangement into two-dimensional sheets – membranes. The environment in which the polymer is immersed, the solvent and its pH level, may modify many properties of the system. Different environments, or polymerization procedures may "charge" the polymer in different ways. This may lead to different excess charges along the chain, with sequences that are either quenched (charges are fixed in place) or annealed (they may exchange places along the chain) [5, 6].

The details of our specific model, the different ensembles studied and the interactions studied are elaborated on separately in Section 3.

1.2 Proteins

Because the relevance to biological proteins is one of the main motivations for the research in this field we now discuss some of their basic concepts and their physical aspects.

Proteins are biological polymers whose monomers are the 20 naturally occurring amino acids. They are part of many structures appearing in biological systems such as hair, bone and cellular membranes. They also take part in many of the biological processes in such organisms, serving as catalysts and regulators for them (enzymes) or transporters of molecules (ion channels, protein motors, etc.) [7].

Proteins differ in their internal construct and sequence of the amino acids forming them. This is known as the *primary structure*. A protein may arrange itself into more complex conformational structures such as α-helices (mostly known from the DNA structure) and β-sheets – called *secondary structures*. These, may in turn, fold into large scale structures, fitting together into globular shapes termed *tertiary structure*. Each globular protein has a unique tertiary shape, also known as its *native state*, dependent on its primary structure. The native state of the protein has a great part in determining its biological function.

Under normal conditions (body temperature, neutral pH) proteins are found in their native state. Irregular conditions may "unfold" the protein into an ensemble of more expanded or *denatured* states. The process of folding into the native state is a question of great interest and has been subject to numerous studies ([4, 7, 8] and references therein). The mechanism by which a protein finds its native state in the exceptionally large phase space is still not fully resolved. The main underlying driving forces and their effect have,

yet, to be determined. This is of great importance in understanding the relation between the amino acid sequence and the protein's function.

Due to the exceptional complexity of this problem, many simplified models have been suggested in an attempt to reveal the underlying relevant mechanisms governing the behavior of this system. Many of them model the monomers to units of a simple monomer-solvent interaction (either solvophobic or solvophylic) or a monomer-monomer interaction of some basic attraction to allow folding. Most of these models restrict themselves to short-range interactions.

Under normal physiological conditions several amino acids have an excess charge[9]. Three are basic and are positively charged (Arg, Lys, His) while two are acidic, thus negative (Asp, Glu). Two others (Cys, Tyr) may become positive under more extreme conditions. These amino acids are not rare: In an average protein, each of them may constitute $2-7\%$ of the primary sequence (the other amino acids have a similar frequency of occurrence) [9]. This means that electrostatic interactions exist in common proteins and may come into play in the folding process. On short length scales this interaction would compete with hydrogen or sulfur bonding and hydrophilic/phobic interactions. On large length scales, characteristic of the protein in its denatured state, it could be assumed to be dominant (disregarding screening) and may determine the onset of folding.

We study the effect of the Coulomb interaction in a simplified system in attempt to understand the main features of this problem as relying on its electrostatic features.

A question of great interest is the dynamic nature of protein folding. The disorder of the complex system may give rise to an energy landscape of a "glassy" nature, leading to a freezing transition to a non-native state. We will address this question in our study, as well, in the context of the electrostatic interactions.

1.3 Two-Dimensional Systems

We investigate a 2-dimensional (2D) charged system where the Coulomb interaction (also 2D) takes a logarithmic form, whose properties are discussed in the following chapters.

There are no real systems that exhibit these properties. There are systems restricted to a 2D plane, but, once charged, these are real charges with a 3-dimensional (3D) interaction. On the other hand, there are systems that display a two charge-type logarithmic interaction (spin vortices, crystal dislocations, etc') but there is no case where these "charges" are polymerized.

Still, there are several reasons why the understanding of real, 3D PAs may profit by turning to a 2D model, as we do:

- When studying critical phenomena, it is, in many cases, favorable to study the problem in general dimensions. Many properties are found to be strictly dimension dependent, so finding the general d behavior is helpful to extrapolate or verify various results.

- It has been stated [10] that many properties of polymer systems are dependent on the surface to volume ratio of the system – condensation energy, surface tension and surrounding conditions compete in determining the shape of the polymer. This ratio is N-dependent. The ratios characteristic of real life 3D polymers ($10^2 - 10^5$ monomers), that can not be numerically studied, are reached in two dimensions for polymers of much shorter lengths, nearing those investigated here.

- Computational complexity: Various schemes of numerical investigation, such as the one employed in this study (exact enumeration) have an exponential complexity that grows with the dimension. Performing such calculations on lower dimensional systems allows shorter running time or the investigations of more elaborate systems (pertaining results are applicable to higher dimensions).

- A similar 3D model has been studied by Kantor and Kardar [11]. Results are not always conclusive, partially due to the previous argument. In 2 dimensions we might hope that some features will be more pronounced allowing a better understanding.

2 Theoretical Review

We now present a theoretical review of topics that are relevant to the understanding of the system studied. We quote known results and concepts that will allow a physical perspective of the model and hopefully provide some intuition as to the questions raised and the results we obtain.

We begin with a discussion of polymer models starting with the basic concepts and gradually enter more complex effects into the problem. Because our main interest is in the Coulomb interaction, we devote a special section to its behavior in two dimensions which is not trivial. Results in 3D are not, generally, applicable to 2D.

2.1 Polymer Models

The discussion here relies greatly on the books by de Gennes[2], Grosberg and Khokhlov[3], and Plischke and Bergerson[12]. See them for a more detailed discussion.

2.1.1 Definitions

We begin with a set of monomers constructing a polymer chain. The polymer will be assigned a set of N displacement vectors $\{\mathbf{a_i}\}$, designating the distance between two connected monomers along the chain:[1]

$$\mathbf{a_i} = \mathbf{R_i} - \mathbf{R_{i-1}} \ ; \ i = 1, ..., N \ , \tag{2.1}$$

where $\mathbf{R_i}$ is the location of the i'th monomer with respect to some origin.

The simplest means of describing the size of the polymer is the *end-to-end vector*:

$$\mathbf{R_{ee}} \equiv \mathbf{R_N} - \mathbf{R_0} = \sum_{i=1}^{N} \mathbf{a_i} \ . \tag{2.2}$$

A more robust measure of polymer size is the *radius of gyration* – R_g, defined by:

$$R_g^2 \equiv \frac{1}{N+1} \sum_{i=0}^{N} \left(\mathbf{R_i} - \mathbf{R_{cm}}\right)^2 = \frac{1}{(N+1)^2} \sum_{i<j} \left(\mathbf{R_i} - \mathbf{R_j}\right)^2 \ , \tag{2.3}$$

where $\mathbf{R_{cm}}$ is the location of the center of mass. This is the length one would measure when performing elastic light-scattering experiments on polymer solutions [3].

[1] In accordance with the references given, we will take here the chain to have $N+1$ monomers, labeled $0, ..., N$. Its length is N steps.

One may obtain a more intricate description of the spatial extent of a specific configuration of the polymer using the *shape tensor*, defined in a 2D space by:

$$S = \begin{pmatrix} \langle x^2 \rangle - \langle x \rangle^2 & \langle xy \rangle - \langle x \rangle \langle y \rangle \\ \langle xy \rangle - \langle x \rangle \langle y \rangle & \langle y^2 \rangle - \langle y \rangle^2 \end{pmatrix} , \tag{2.4}$$

where $\langle ... \rangle$ denote averages taken over the coordinates of all monomers. The two eigenvalues of the shape tensor – λ_1, λ_2, describe the size in the direction of the two principal axes[2]. Taking $\lambda_1 < \lambda_2$, we define the *axial ratio* $\equiv \lambda_1/\lambda_2$. The axial ratio ranges between 0 (elongated shape) and 1 (non elongated shape). It is easy to show that:

$$R_g^2 = Tr\{S\} = \lambda_1 + \lambda_2 \ . \tag{2.5}$$

2.1.2 The Ideal and Gaussian Chains

A simple realization of a polymer could be that of equally separated monomers, with $|\mathbf{a_i}| = a$, free to turn in any direction at each step – referred to as a *freely jointed chain* or an *ideal chain*. This is practically a random walk progression. Assuming all steps are independent, the natural random walk result is obtained:

$$\left\langle \mathbf{R}_{ee}^2 \right\rangle = Na^2 \ . \tag{2.6}$$

It is also easily shown for the radius of gyration [12]:

$$\left\langle R_g^2 \right\rangle \simeq \frac{Na^2}{6} \ . \tag{2.7}$$

These results may be stated more generally in the form:

$$\left\langle \mathbf{R}_{ee}^2 \right\rangle \sim \left\langle R_g^2 \right\rangle \sim N^{2\nu} \ . \tag{2.8}$$

Restricting the walk to a lattice or to limited angle rotations does not change the scaling exponent. In the thermodynamic limit ($N \to \infty$), the chain will have a Gaussian extension:

$$p(\mathbf{R_{ee}}) \propto N^{-d/2} e^{-d\mathbf{R}_{ee}^2/2Na^2} \ , \tag{2.9}$$

where d is the space dimension of the lattice.

[2]Note that the λs are "squared distances".

A similar result may be retrieved using a more generalized and a somewhat more realistic model of the polymer – the *Gaussian chain*: Following Eq. 2.9, the set of separation vectors $\mathbf{a_i}$ are no longer restricted to a magnitude a but are assigned a Gaussian probability:

$$P(\mathbf{a_i}) \propto e^{-d\mathbf{a_i}^2/2a^2}. \tag{2.10}$$

The distribution of R_{ee}, which is the product of the probabilities for the individual $\mathbf{a_i}$, summed over all possible sets, will match that of Eq. 2.9.

Should we formally write the expression for the probability of a given configuration, $P(\{\mathbf{a_i}\})$, this could be interpreted as a Boltzmann weight factor with an effective Hamiltonian:

$$H = \frac{dk_BT}{2a^2}\sum_{i=1}^{N}(\mathbf{R_i} - \mathbf{R_{i-1}})^2 \ . \tag{2.11}$$

For a continuous chain, not one of discrete monomers, a continuous limit for the above equation may be derived:

$$H = \frac{dk_BT}{2a^2}\int_0^N \left(\frac{d\mathbf{R}}{ds}\right)^2 ds, \tag{2.12}$$

with s being an internal coordinate along the chain.

This Hamiltonian may be interpreted as being of an elastic origin, with an effective "spring constant" expressing the chain's "entropic resistance" to extension or what is known as *entropic elasticity*.

Accordingly, following the definition of the probability, terms describing the entropy or free energy of the chain may also be derived. The Hamiltonian written above assumed no interaction between the monomers and describes only the statistical aspects of a random walk. In the following sections this Hamiltonian will serve as a basis for extensions when introducing more elaborate interactions.

Going back to the ideal chain, if it is restricted to a lattice, we may define $\mathcal{N}(N)$ as the number of different walks for an N-step chain. In the case of an ideal random walk we may easily see that

$$\mathcal{N}^{RW}(N) = z^N \ , \tag{2.13}$$

where z is the *coordination number* of the lattice – the number of different steps the walk can take from a certain site. For a 2D square lattice $z = 4$.

2.1.3 Excluded Volume Effects – Self-Avoiding Walks

The next step in trying to model a real system is to introduce excluded volume effects. A real polymer cannot self intersect. There is a hard-core repulsion that prevents two particles from coming closer than a minimum hard-core radius.

The Gaussian-model Hamiltonian (Eq. 2.12) may be generalized to describe this by adding a two-body exclusion term:

$$\beta H = K \int_0^N ds \left(\frac{d\mathbf{R}(s)}{ds} \right)^2 + \omega \int_0^N ds \int_0^N ds' \, \delta^d \left(\mathbf{R}(s) - \mathbf{R}(s') \right) \ , \tag{2.14}$$

where s is an internal coordinate along the chain.

A polymer with excluded volume is modeled by the concept of a *self-avoiding walk* (SAW), where a natural scheme would be that of a SAW on a lattice. This reduces, inevitably, the number of walks a polymer chain may assume and its spatial extent is, on the other hand, increased.

The total number of SAWs for an N-step long chain is asymptotically [2]:

$$\mathcal{N}^{SAW}(N) \propto \overline{z}^N N^{\gamma - 1} \ , \tag{2.15}$$

where $\overline{z}$ is the effective coordination number of the lattice and γ is a dimension-dependent exponent. For a hypercubic lattice [13]: $\overline{z}^{2D} = 2.64$, $\overline{z}^{3D} = 4.68$. This may be compared with the ideal result (Eq. 2.13): $z^{2D} = 4$, $z^{3D} = 6$. For two dimensions $\gamma \simeq 4/3$ [2]. For such a chain, with no other interactions besides the restricted volume, the end-to-end distance, as the radius of gyration, has a mean square average that scales like:

$$\left\langle \mathbf{R}_{ee}^2 \right\rangle \sim \left\langle R_g^2 \right\rangle \sim N^{2\nu} \ , \tag{2.16}$$

where ν is another universal scaling exponent [2]:

$$\nu(1D) = 1 \ ; \ \nu_F(2) = \frac{3}{4} \ ; \ \nu(3D) \simeq 0.588 \ . \tag{2.17}$$

These results may be derived, to a very good accuracy, using the Flory approximation [1].

2.1.4 The Θ-Transition

A real polymer system is subject to other interactions on top of those mentioned above. Usually we expect some longer range interaction of a van der Waals type between monomers.

This interaction will usually be mediated by the solvent surroundings. Solvents are categorized as *good solvents*, in which the attraction between the monomers and solvent is stronger than that between the monomers themselves, causing an expansion, and *bad solvents*, in which the intra-monomer attraction is more dominant, leading to contraction.

Temperature, solvent conditions and interaction strength could mediate a net attractive interaction between monomers which rivals the excluded volume restriction. We can distinguish between two regimes: At high temperatures most interactions become irrelevant, except for the excluded volume and we expect a SAW behavior, as described in the previous section. At very low temperatures, the attractive forces may dominate and the polymer collapses into a dense, compact configuration with a spatial extent of $R_g \sim N^{1/d}$. Between these two regimes, there is a transition at a temperature denoted as the Θ temperature and, hence, the term Θ-*transition*. At the transition point itself there is an effective cancelation of the two competing interactions which leads to the disappearance of the second virial coefficient. In three dimensions this results in an ideal random-walk at the Θ-point with $R_g \sim N^{1/2}$.

This transition has been subject to extensive study and it is understood to be a *tricritical phase transition* [12, 14]. For polyampholytes it has been shown [15] that below 4 dimensions, electrostatic interactions are a relevant parameter. PAs in 2D belong to a different universality class and will not undergo a Θ-transition. There is, however, a collapse phenomenon of a different nature, which is described in the following chapter.

2.1.5 Polyampholytes

Electrostatic charges may be added to the monomers, which become subject to long-range Coulomb interactions. The treatment of such polyampholytes is much more complicated than polymers with neutral, short-range interacting monomers. The application of many theoretical methods is complicated.

Edwards *et al.*[16] and later Higgs and Joanny [17] stated that the charge fluctuations along a neutral PA create a weak net attraction. Upon lowering the temperature, the PA should collapse into a *dilute globular* state, with a density much lower than that of a closed packed configuration. They assume that in this dilute state the PA can be treated like an electrolyte solution as described by the Debye-Hückel formalism [18]. The chain is at thermal equilibrium and can easily change its configuration. There is enough freedom for the polymer to re-arrange its charge distribution so the electrostatic interaction is

screened thus lowering the energy in the collapsed state. A sufficiently long neutral PA will be collapsed at all temperatures.

The resulting picture can be described as a chain of "blobs": For short parts of the chain the charge fluctuations and the related electrostatic energy are small. They will be temperature-dominated and their statistics will be of a SAW. These segments form dilute blobs with a typical size of the Debye-Hückel screening length – this is the size above which the electrostatic energy dominates over the thermal. These blobs can be considered as the new renormalized charges or monomers. Between them there will be a screened electrostatic interaction, so they will form a close packed arrangement. The collapse is not a sharp phase-transition. As temperature decreases, the Debye-Hückel screening length shortens creating smaller blobs and a more compact globule.

Victor and Imbert [19] claim on the basis of numerical simulations that a PA with a sequence of alternating sign charges, which is locally neutral, will behave like an overall neutral polymer in a poor solvent with a short-range attractive interaction. This leads to the regular Θ-transition and is in disagreement with the prediction of the collapse thru the Debye-Hückel theory. A theoretical discussion by Wittmer *et al.* [20], based on the random phase approximation, resolves the contradiction by introducing the charge correlations along the chain as an important parameter in determining the properties of the PA. This allows the recovering of both results for the random and correlated sequences.

A different view has been taken by Kantor, Kardar and Li [11, 21, 15, 22, 23] that study the problem of a randomly charged PA both theoretically and numerically. Generalizing the Hamiltonian of an excluded volume polymer (Eq.2.14) to include the Coulomb interaction, we get:

$$\beta H = K \int_0^N ds \left(\frac{d\mathbf{R}(s)}{ds} \right)^2 + \int_0^N ds \int_0^N ds' \left[\omega \delta^d \left(\mathbf{R}(s) - \mathbf{R}(s') \right) + \frac{\beta}{2} \frac{q(s) q(s')}{|\mathbf{R}(s) - \mathbf{R}(s')|^{d-2}} \right] . \tag{2.18}$$

Applying scaling relations, Kantor *et al.* [15] conclude that $\nu = 1/(d-2)$. That is, in 3 dimensions the PA is fully stretched. This does not contradict Higgs and Joanny [17], whose treatment within the Debye-Hückel formalism requires absolute neutrality of the system, but points to the importance of the ensemble or preparation of the system. Numerical studies of this system [11, 22] support these statements.

A PA is defined to have an excess charge $Q = (N_+ - N_-)q_0$, where $N_+(N_-)$ is the number of positive (negative) charges of magnitude q_0. The properties of a PA should

depend on this parameter. A randomly charged PA will have a typical excess charge of $Q \simeq q_0\sqrt{N}$.

The effect of excess charge may be such that we can define a critical charge that separates different regimes of behavior. Actually, the full description of a PA compactification requires the definition of two such charges:

- High Temperature Critical Charge – Q_c^H

  At very high temperatures the PA is a SAW. Upon lowering the temperature, the Coulomb interaction comes into play, first as a small perturbation, causing the chain to contract or expand. Most states are still thermodynamically relevant and a minimization of the free energy is required.

  A simple high temperature analysis (see section 4.2) shows that for any space dimension $Q_c^H = q_0\sqrt{N}$. This is also the typical excess charge of a random chain. Chains with an excess charge above this value will expand while those with a lower excess charge will contract.

  This critical charge defines the lowest order behavior in the high temperature limit. Further lowering of the temperature introduces higher order terms that come into play. The process is *not* monotonic expansion or contraction all the way down to zero temperature.

- Low Temperature Critical Charge – Q_c^L

  At very low temperatures, the PA will settle into the most energetically favorable configuration, regardless of entropy considerations. The critical charge in this case is not the same as in high temperatures.

  The critical excess charge for this case was calculated by Kantor and Kardar [22] by analogy to Rayleigh's charged drop model: We assume a condensed spherical shape, with the excess charge evenly distributed in the drop. Above a certain excess charge, the "Rayleigh charge" – Q_R, the outward pressure of the Coulomb repulsion exceeds the inward pressure of the surface tension. This will create a local instability of the drop to elongation. For general dimensions

  $$\Delta p = 0 \Rightarrow Q = Q_R \sim N^{1-3/2d} \ , \tag{2.19}$$

  where Δp is the pressure difference at the surface of the drop. The derivation of the 2D case is presented in section 4.1.1.

Even before the drop becomes locally unstable, a global instability may appear – it may be energetically favorable for the charged drop to split up into smaller distant droplets. The critical charge will then, generally, be $Q_c^L = \sqrt{\alpha} Q_R$. In 3D $\alpha = 0.293$ [22].

Chains with an excess charge beneath the critical value will have a compact ground state (analogous to a condensated drop). Higher excess charge will lead to an expanded ground state (analogous to the disintegration of the drop into smaller droplets). The arising picture is described as the *necklace model* [22]: Because a real chain cannot break up into disconnected, distant droplets, segments with $Q < Q_R$ form compact beads connected by highly charged, extended strands. The shape is overall extended. The competition between the gain in energy by breaking up into beads and the cost in surface tension of the strands connecting them, determines the rate of expansion.

Only in three dimensions do Q_c^L and Q_c^H scale the same with N. Generally, at intermediate temperatures, R_g does not change monotonously.

Gutin and Shakhnovich [24] also describe an expansion when lowering temperature due to a large excess charge. However, in their view the globule, still composed of thermal blobs, becomes more elongated. Dobrynin and Rubinstein [25] apply a modified Flory theory to include the Coulomb interactions. They discriminate between three temperature regimes: (1) A high temperature *unperturbed regime*. (2) An intermediate temperature *polyelectrolyte regime* dominated by the excess charge. The chain may expand or collapse when reducing temperature. (3) A low temperature *polyampholyte regime* where charge fluctuations always cause a reduction in size. The excess charge determines the aspect ratio of the globule. A highly charged chain will still compactify at low temperatures, but with an elongated aspect ratio.

Levin and Barbosa [26] suggest that there exists an even lower temperature phase, resembling an affine network or a microgel, more expanded than the dilute globule, with $\nu = 2/5$ in three dimensions. This will, upon raising the temperature, collapse into the dilute globule state. They also speculate that the system may undergo a glass transition at these low temperatures and get trapped inside some metastable energy minima. Victor and Imbert [19] also suggest that there might exist a *critical degree of disorder* of the charge sequence along the PA: Below it the transition is merely a Θ point, above it they

expect a glass transition.

2.1.6 The Freezing Transition

Heteropolymers, as many other disordered systems, may exhibit a freezing phenomenon. A dynamic description of such a transition would mean that the system relaxes into a state other than its ground state. For a random system, apart from the low energy unlocalized excitations (such as phonons), other low energy excitations may exist in configurations that are "far away" in the energy landscape from the ground state and may have high energy barriers separating them. Once caught in such a state, a local energy minima, the system will have a very low probability of escaping it and finding the global minimum, thus freezing.

Thermodynamically viewed, this transition may be described as an *entropy crisis*: Below a certain temperature, the number of states accessible to the system drastically falls off from a macroscopic value to some very small number of deep minima configurations, each with very little entropy. The system will freeze into one of these meta-stable states, depending on the "cooling history", very much like a glass.

The freezing transition is frequently described in the terms of the *random energy model* (REM) applied by Derrida to spin glasses [27, 4]. One of the model's main requirements is a statistical independence of states. A very rough energy landscape is generated by assigning each state a random energy by some Gaussian distribution function. As a result, "nearby" states do not have similar energies and vice-versa. Moreover, the low energy tail of the energy distribution falls off dramatically so as to cause the entropy crisis at some low temperature. A system obeying the REM conditions is expected to exhibit the freezing transition.

The random energy landscape is very much a result of the disorder of the system which leads to *frustration*. The heterogeneity of the system, the number of monomer types and their sequence in a polymer system for example, may contribute to this frustration and affect the appearance of a freezing transition.

Most studies concerning the existence of a freezing transition in heteropolymers considered short-range interacting models [28, 29, 30, 31, 32, 33, 34]. In some cases they do find evidence of a frozen state at low temperatures. These references verify the existence of a freezing transition by studying several thermodynamic variables that try to measure the relevant properties characterizing a system that undergoes freezing. In section 4.6 we

study these indicators, adapted for the long-range Coulomb interaction to investigate the possibility of such a transition in the present context.

Short-range interacting systems seem to be likely candidates for a freezing transition. Simple changes in their configuration may change their energy drastically, as expected by REM. Long-range interacting systems seem less so. The system cannot "hide" charges from others and energies are likely to be correlated, in violation of REM [35]. However, as noted when discussing PAs, some authors do speculate that they might undergo a freezing transition at low temperatures [19, 26].

2.2 Two-Dimensional Electrostatics

2.2.1 The Coulomb Interaction

The Coulomb potential is the solution of the Poisson equation: $\nabla^2\phi = -\Omega_d\rho$, where Ω_d is the solid angle of a d-dimensional hyper-sphere. When solving for a general dimension d, the potential created by charge q at a distance r is:

$$\phi^{d\neq 2}(r) = \frac{q}{r^{d-2}} \ . \tag{2.20}$$

The 2D space (which can be described as infinitely long, parallel wires with a constant charge density along them in real space) has a different solution:

$$\phi^{d=2}(r) = -q \ln \frac{r}{r_0} \ , \tag{2.21}$$

where r_0 is a constant defining the reference point (we return to this point, in greater detail, later on in this chapter).

The logarithmic behavior gives rise to many peculiar results. The interaction diverges logarithmically with no finite bound. When discussing the energy of a system of charges, one cannot define it as the energy required to assemble the system by bringing the charges from an infinite distance — energies will diverge. In our study this manifests itself in the questions regarding the definition of the energy of the system. Because the interaction changes slowly with the distance, slower than the $\frac{1}{r}$ behavior in three dimensions, it is not obvious that energies converge in the thermodynamic limit, when the size of the system is taken to infinity. The interactions are certainly not local, making the results very much susceptible to long-range effects like the surface conditions.

Similarly, excess charge will have a pronounced effect on the system. Unlike in a 3D system, where "like-charges" can gain only a finite energy by separating themselves as far

away from each other as possible, in 2D they can gain an infinite energy. This inevitably affects the spatial extent of the polymers studied here and their critical charge.

Throughout this work we will tackle some of the problems mentioned here that are pertinent to understanding the results obtained using simulations for finite systems and their applicability to the thermodynamic limit. In this case, the logarithmic behavior poses a special difficulty. The slow variation of the energy makes the leading behaviors and divergences, if they occur, evident only over several orders of magnitude.

2.2.2 The Two-Dimensional Coulomb Gas

We study a polymer, i.e. charges are connected together in a flexible chain. However, all possible configurations of the chain are a subset of the configurations accessible to free charges. At certain conditions the chain may exhibit behavior similar to that of the gas. A chain long enough, whatever the specific sequence of charges along its backbone, might be able to assume any charge-space configuration with statistics like that of the gas. This is the assumption that allows the description of the dilute globular PA (section 2.1.5) as an electrolyte fluid. Understanding the behavior of the 2D Coulomb gas may help to point out what type of behavior to expect for our polymer system.

A 3D gas of charged hard spheres is known to undergo a gas-liquid phase transition. At certain conditions it is noted by a discontinuity in the density of the "fluid" [36]. The critical behavior of this transition has not been, yet, fully determined. A possible crossover to the asymptotic critical behavior appears unusually close to the critical point. It has been speculated that $d = 2$ is a marginal dimension for this system [37].

Much work has been devoted to the study of the 2D Coulomb gas ([36, 38, 39, 40, 18, 41] are a few starting points). We will concentrate on the relevant results for a neutral gas.

High Temperature Limiting Behavior: For a neutral fluid of point-like ions, scaling relations allow an exact derivation of an equation of state [42]:

$$\frac{p}{\rho k_B T} = 1 - \frac{T_0}{T} \ , \tag{2.22}$$

where $T_0 = \frac{q^2}{4k_B}$ is the Kosterlitz-Thouless temperature (see below), p is the pressure and ρ is the particle density. This equation is valid for $T > \frac{q^2}{2k_B}$. Although no proof has been provided, this result is reasonable for hard-core particles as well, in the low density limit [42].

At the infinite temperature limit the interaction energy is irrelevant and all possible states are equally probable. The Coulomb gas will then behave as an ideal gas, possibly with hard-core repulsion. A polymer does not have the freedom of the gas particles and at such temperatures it will have a SAW behavior instead.

For the Coulomb gas, the first correction, when lowering the temperature, is calculated within the framework of the Debye-Hückel approximation. The calculation, assuming a self-consistent re-distribution of charges in space under the influence of the interaction, results in a screened potential: At large distances from a certain charge, the potential dies out exponentially with a characteristic length scale. In two dimensions we get [18]:

$$\phi(r) \sim \frac{q}{\sqrt{r/b}} \cdot e^{-r/b} \ , \tag{2.23}$$

where

$$b^2 \equiv \frac{k_B T}{4\pi\rho q^2} \ . \tag{2.24}$$

A neutral PA, as described in section 2.1.5, collapses into a dilute globular state. If in this compact but dilute phase, the chain has enough freedom to re-arrange its charge distribution its features may be described in the terms of a Debye-Hückel screened liquid.

Low Temperature Limiting Behavior: At very low temperatures the 2D neutral Coulomb gas undergoes the known Kosterlitz-Thouless transition [38]. Pairs of opposite charges condense into neutral dipole pairs, behaving as an insulating gas of weakly interacting dipoles with a finite dielectric constant. Above the transition temperature T_0 the pairs will start breaking up into separate charges and the conducting, screened phase will appear[3].

For a discrete system with charges restricted to a lattice, Lee and Teitel [43] presented the full phase diagram that has two low temperature phases: At low densities there is a gas phase of neutral bound pairs. As density increases there is a first order transition to an insulating "checkerboard" state (which we will refer to as a salt crystal).

For the polymer system, the collapsed compact globule at low temperatures may correspond to the high density limit[4]. Of course, the polymer bonds prevent folding

[3]By "screening" we mean an exponential dying of the potential which is possible only for the free charges. This is opposed to the low temperature state where the dipoles can only create a finite dielectric constant.

[4]There is no direct correspondence to the model of Lee and Teitel [43] which is for an ensemble defined by an average number of particles, unlike our constant length chain.

exactly into the salt crystal state, but, there are some conclusions to be drawn: Since the states accessible by the polymer are a subset of those accessible to the gas, we can see the salt crystal state as a lower bound of our system's energy. We can also expect the alternating charge quench and the annealed ensemble to assume such a ground state since they can access it as well.

The Energy of a System of Charges: If we measure the distances between charges, denoted by l_{ij}, in units of a basic length a, then the energy of a system of charges may be written as:

$$E = -\sum_{<ij>} q_i q_j \ln \frac{l_{ij}}{r_0} = -\sum_{<ij>} q_i q_j \ln r_{ij} \frac{a}{r_0} \ , \tag{2.25}$$

where r_{ij} is now dimensionless and $\langle ij \rangle$ denotes a summation over all charge pairs (i, j). The energy may then be written as the sum of two terms:

$$E = -\sum_{<ij>} q_i q_j \ln r_{ij} - \sum_{<ij>} q_i q_j \ln \frac{a}{r_0} \ . \tag{2.26}$$

If all charges are of the size $\pm q_0$, then for a given excess charge Q the energy may be re-written as:

$$E = -\sum_{<ij>} q_i q_j \ln r_{ij} - \frac{1}{2}\left(Q^2 - q_0^2 N\right) \ln \frac{a}{r_0} \ . \tag{2.27}$$

The first term on the right hand side depends on the charges' space configuration and sign. The second term is a constant, independent of the charge configuration (or sequence along the polymer), and is a function only of the excess charge. Throughout this work we take $r_0 = a$ so the second term falls off and calculate only the first term, calling it the "energy". Within an ensemble of the same excess charge, this has no effect since we are interested only in energy-differences. However, it must be kept in mind that for different excess charges the choice of r_0 sets a different reference point, that scales as N and may change sign.

2.2.3 The 2D salt crystal

This study deals in a large part with low temperature characteristics of the system. The behavior of the 2D gas in this limit, specifically its ground state is of great interest. As mentioned above, the ground state configuration of the 2D coulomb gas on a lattice is that of a salt crystal.

We focus on the energy of the ground state, namely on its being extensive with surface correction terms. In a phenomenological form we would like to express the energy as:

$$E = -\epsilon_c V + \gamma S \ , \tag{2.28}$$

where ϵ_c is the condensation energy and γ is the surface tension. For a 2D system in a compact state, $V \propto Na^2$ (ϵ_c has units of $\frac{q_0^2}{a^2}$) and $S \propto a\sqrt{N}$ (γ has units of $\frac{q_0^2}{a}$). We can, therefore, describe the energy as:

$$\frac{E}{q_0^2} = -A_1 N + A_2\sqrt{N} \ . \tag{2.29}$$

In Appendix A we carry out the detailed proof that there exists an extensive energy for this configuration of charges and the above equations are valid.

The basic problems this derivation deals with are the divergence of the logarithmic interaction and the mathematical complexity of summing up the discrete contributions. The general scheme we apply is to divide the plane into small, repeating, neutral subunits whose interaction is then much weaker (multipole-multipole) and falls of fast enough with distance. At large distances we are able to integrate over a continuous spread of such units enabling the overall calculation.

The total energy of the salt crystal is comprised of several contributions. There is a bulk term, to which we add corrections arising from the boundary effects. These contributions are explained and calculated in Appendix A.

In all, we find that the energy of the ground state of the 2D salt crystal can be considered extensive with surface corrections. However, as pointed out in Appendix A some pathological cases violate this. A "relaxed construction" of such a crystal must be assumed to prevent these cases.

Later on (section 4.1.2) we address this problem numerically, accounting for the whole ensemble of neutral, quenched polymers, not only those that collapse into a salt-crystal like configuration and try to find an extensive description for their energy as well.

3 The Model

3.1 The Two-Dimensional Model Polyampholyte

We study a model of a discrete monomer chain on a 2D square lattice. The distance between connected monomers is restricted to one lattice spacing. The chain is not allowed to intersect or overlap itself, behaving like a self-avoiding walk.

Each monomer has an integer charge of $q_i = \pm q_0$. Charges and space are also 2D, so the pair interaction is the usual logarithmic one:

$$E_{i,j} = -q_i q_j \ln \frac{|\mathbf{r_i} - \mathbf{r_j}|}{r_0} \ . \tag{3.1}$$

The Hamiltonian describing this system is:

$$H\{q_i, \mathbf{r_i}\} = \sum_{\{i,j\}} -q_i q_j \ln \frac{|\mathbf{r_i} - \mathbf{r_j}|}{r_0} \ . \tag{3.2}$$

As discussed previously, we define $r_0 \equiv$ one lattice spacing $\equiv' 1'$. We neglect the contribution due to excess charge that enters by setting the reference point. We will measure temperature in units of the interaction – q_0^2, so q_0^2/T is dimensionless and $k_B = 1$.

Energy terms related to the polymerization, hard-core and self-avoiding potential, are left out since we consider only configurations that comply with these restrictions (they could be defined as contributing zero energy in the allowed configurations and an infinite energy in the restricted ones). We assume the polymer is in a very dilute solvent and neglect any effect it may have in a real system.

When discussing real polymers, an important length scale that comes into play is the *persistence length* or *Kuhn segment*. This is a measure of the chain's stiffness, the segment over which the directions of the individual bonds are still correlated. This can range from single bonds in certain synthetic polymers up to approximately 150 in DNA molecules [3]. It is important to note that in our model the chain is free to bend in any direction at each bond (within the lattice and excluded volume restrictions). So, in some aspects, every "monomer" in our problem represents a much longer segment in a real system. This is important due to the rather short chain lengths we examine in this study.

The three dimensional equivalent of this model has been studied by Kantor and Kardar, using both Monte Carlo [22] and enumeration [11] methods. This study is intended to extend their investigations to longer chains and address some questions they did not.

In two dimensions most studies are limited to short-range interactions. Victor and Imbert [19] studied a Coulomb model restricted to the alternating charge sequence. Golding and Kantor [44] study a short-range model of a "very highly screened" Coulomb potential.

Throughout this work we investigate the behavior of several different ensembles. For each, we were interested in specific questions and values that dictated the method employed. The different cases studied were:

- Quenched Disorder – Charges are fixed in place along the polymer. Thermal averages are calculated for all spatial configurations of a specific charged sequence. Thermodynamic quantities are then averaged over all quenches of the same excess charge. Different excess charges are treated as separate ensembles.

- Alternating and Fully Charged Quenches – These two specific quenches were also studied separately due to special interest in their behavior.

- The Annealed Ensemble – Charges are free to interchange positions along the chain but, still, with an overall constraint on the excess charge. For this ensemble we studied the details of the ground state only, which is simply the lowest of all ground states of all quenches with the same length and excess charge.

For such ensembles our control parameters are the excess charge on the chain – Q measured in units of q_0 (whose notation we omit at times) and the temperature – T. Their influence on the various properties (energetic and spatial) of the polymer were studied. We vary the total number of monomers/charges in order to extrapolate the behavior at the thermodynamic limit.

We studied polymers of up to 26 monomers long. Up to length 18 the enumeration was exhaustive of all possible charge sequences. Above this, random samples were investigated. For each quench, all spatial configurations were enumerated and thermal averages of the relevant thermodynamic variables were taken. 1000 temperatures were considered between 0.01 - 10 in 0.01 steps.

3.2 The Numerical Method

Enumeration

For the model investigated we chose to use the scheme of exact enumeration, i.e. creating and calculating rigorously values for all possible realizations of the ensemble under

question. This way the exact partition function could be evaluated and, hence, all the thermodynamic variables related to it.

The enumeration method used a recursive depth first algorithm: From the origin we advance along the lattice in single, discrete steps forming a path. Whenever the required extent of the chain is reached, or advance is blocked by the chain self-intersecting (thus violating the SAW restriction), the path retraces itself to the closest possible lattice-node along its course and tries to advance in a new direction. This goes on until all possible options are exhausted, ensuring that all possible SAWs of a required length are created. Each time a path of the full required length is obtained (N monomers, $N-1$ steps) that configuration's relevant values are calculated and added to the statistical averages.

Derivation of exact values through exhaustive search is most important when investigating low temperature behavior and the ground states of a system. Monte Carlo techniques fail to equilibrate and produce correct results at these conditions. Since this research deals with many low temperature effects (the shape transition, possible freezing and ground state structure) the enumeration technique is the most appropriate.

The main drawback of such a method arises from complexity considerations. The number of SAWs on a 2D square lattice grows asymptotically as 2.64^N (see Eq. 2.15). The total number of quenches for a given length grows as 2^N. In all, this defines an exponentially growing complexity for the complete enumeration.

Reflection and rotation symmetries allow actual enumeration of about $\frac{1}{8}$ of all SAWs for a given length. Charge conjugation and sequence reversal symmetries enable the enumeration of only about $\frac{1}{4}$ of all quenches of a given length. See Appendix B for the exact considerations and actual numbers of quenches and configurations enumerated.

Due to the long-range Coulomb interaction, calculation of the energy for a given sequence and configuration is of N^2 complexity. This is the main computational difference from short-range interactions.

All these restrict the investigation to relatively short lengths compared to natural polymers and to those obtained using Monte Carlo methods. For comparison we might note that the longest sequence enumerated here was 26 monomers long, while using MC techniques for a 2D Coulomb interaction model Victor and Imbert [19] studied a single, 200 monomer long, sequence.

Thermal averaging of all different configurations adds the number of different temperatures evaluated as a multiplicative factor in the complexity. Basically the temperature-

step was such that all features of the different curves could be examined accurately, mainly the low temperature effects. It was not changed in the different simulations, but similar calculations for longer chains (where lattice discreteness is less pronounced) might require finer temperature detail.

Calculation of Values

While enumerating all configurations of a certain quench, the values of certain variables of interest were calculated for each configuration. These were added to histograms whose cells correspond to the energy value of the specific configuration. The histograms served for calculating the partition function and the different thermal averages at the requested temperatures.

The histogram method reduced the thermal averaging calculations to the number of cells in each histogram (C=8192) instead of the total number of configurations ($\sim 2.6^N$). For example, the thermal average of a variable X was calculated like this:

$$Z = \sum_{i=1}^{\text{conf}} e^{-\beta E_i} \ , \tag{3.3}$$

$$\langle X \rangle = \frac{1}{Z} \sum_{i=1}^{\text{conf}} X_i e^{-\beta E_i} = \frac{1}{Z} \sum_{E_j=E_1}^{E_C} \left[\sum_{i=1}^{\text{conf}} X_i \delta(E_i - E_j) \right] e^{-\beta E_j} \ . \tag{3.4}$$

As mentioned earlier, final results, concerning ensembles of several quenches, were obtained by algebraically averaging these calculations over all quenches in the ensemble.

The interaction energy is continuous and does not have any characteristic energy scale. Therefore, the determination of the minimal bin size in the histogram was not obvious. For the lengths fully enumerated, the minimal and maximal energies for each quench were first found and histogram bounds were set accordingly to ensure optimal exploitation of all bins. The number of bins (8192) was set, after studying the low energy tail of the energy distribution for various quenches, so we could distinguish well between the discrete states there. This was important due to our interest in low temperature behavior. The minimal temperature and increment size were also set to 0.01 according to this reasoning.

While scanning all configurations, details of the ground state were also obtained, for each quench. These were used separately for the relevant calculations and are exact (as opposed to histogram-related calculations).

4 Theoretical and Numerical Results

4.1 Low-Temperature Properties

We begin the investigation of the system with a study of its ground state properties – its shape and energy features. This is the state to which the polymer relaxes at low temperatures and is important in setting a reference point with which high temperature properties may be compared.

If the ground state is compact then we would like to express its energy in a phenomenological form (generalizing Eq. 2.28) consisting of condensation energy, surface tension and electrostatic energy terms:

$$E = -\epsilon_c V + \gamma S - Q^2 \ln R \ , \tag{4.1}$$

where Q is the excess charge and R is a characteristic measure of the size.

In the following section we study the shape of the ground state to see if and in what cases it is compact and the above form could be applied. As a consequence, we apply this description to neutral quenches (that do not have an overall electrostatic term). We then check the effect on this picture of introducing excess charge.

4.1.1 Critical Charge

The discussion of PAs (section 2.1.5) led to a definition of a low temperature critical charge – Q_c^L, that describes the chain's low temperature state: expanded or contracted. We now follow the analogy to the Rayleigh drop model by Kantor and Kardar [11, 22] and derive the value for two dimensions: Assuming a conducting charged drop has a circular shape of radius R, we model the non-extensive contribution to the energy as

$$E = 2\pi R\gamma - \frac{1}{2}Q^2 \ln R \ , \tag{4.2}$$

At some critical excess charge the drop will become unstable due to the electrostatic pressure. Differentiating the energy with respect to R, we find the pressure difference at he surface of the drop:

$$\Delta p = \frac{1}{2\pi R}\left(2\pi\gamma - \frac{Q^2}{2R}\right) \ . \tag{4.3}$$

At the Rayleigh charge the pressure difference vanishes, thus we get

$$\Delta p = 0 \Rightarrow Q_R^2 = 4\pi\gamma R \ \Rightarrow \ Q_R \sim N^{1/4} \ . \tag{4.4}$$

At this point the drop is locally unstable to elongation. However, the energy gain by breaking up the drop into two separate droplets may create a global instability at a lower excess charge. The 2D logarithmic interaction creates an anomaly. Because it has no asymptotic finite boundary, for any minute excess charge it is always favorable to break up into distant droplets. This is analogous to the polymer expanding. Thus, the low temperature critical charge in two dimensions is $Q_c^L \to 0$.

Another argument is that opposite charges pair together into weakly interacting dipoles. A single excess charge, that does not pair up, will not cause repulsion, but any excess charge above that will. This leads to a critical charge of q_0. Both arguments imply an N-independent critical charge, but seem to be more applicable to a fluid than to a quenched polymer. We now check how our model system behaves.

All quenches of lengths of 6–18 monomers were investigated. First, for clarity, we display in Figure 1 the temperature dependence of R_g^2 for all ensembles of different excess charges (specifically for an 18 monomer long chain). Two types of behavior are evident: At high enough temperatures all chains approach the SAW limiting behavior. Upon lowering temperatures, excess charge decides between expansion or contraction. At zero temperature it is the low temperature critical charge – Q_c^L that separates between the ensembles that settle to a compact ground state (the lower curves in the graph) or an extended one (the upper curves).

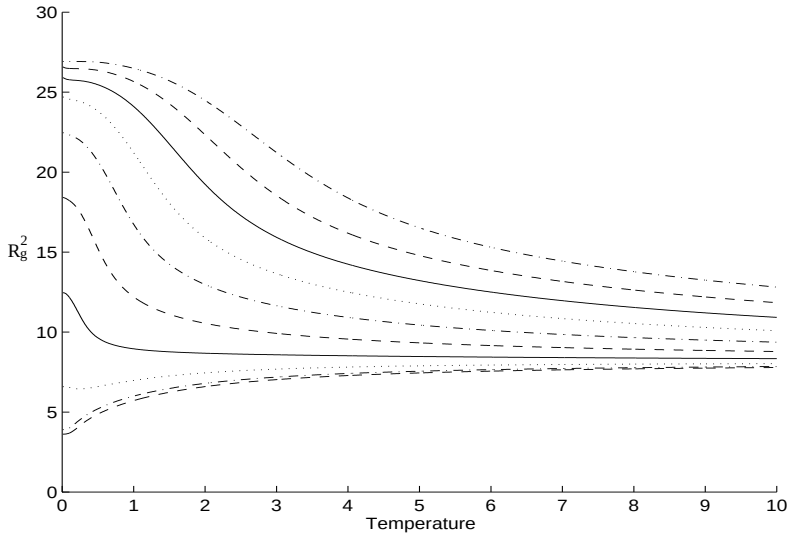

Figure 1: R_g^2 *vs.* Temperature for a 18 monomer long chain. Excess charge is $Q = 0, 2, 4, ..., 18$ from bottom to top.

We see in Fig. 1 that for $Q \leq 4$ the ground state is more compact than the high-

temperature SAW. Above this value it expands. This behavior, with this specific value, repeated itself for all the lengths examined. This might suggest that there is a constant critical charge $Q_c^L = 4q_0$.

However, a compact shape is defined by its scaling with respect to N, not by its actual size. For a compact shape, we expect $R_g^2 \sim N$. An expanded shape is defined by $R_g \sim N$ and the axial ratio $\lambda_1/\lambda_2 = 0$. Figure 2 depicts different low temperature ($T = 0.01$) spatial properties of the polymer for different lengths as a function of excess charge. We display R_g^2/N which should be an N-independent constant up to the critical charge and the axial ratio that should drop to zero at the critical charge.

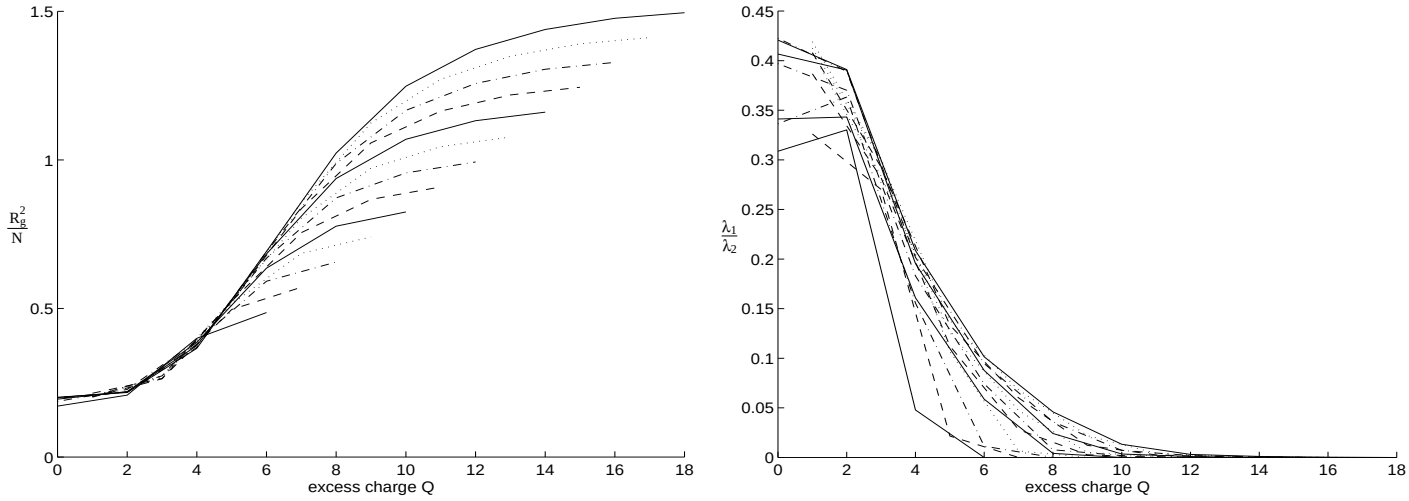

Figure 2: Left: R_g^2/N *vs.* Q. Curves are for different lengths (N=6,7,..,17,18 from bottom to top). Note the collapse of the curves at low Q and their deviation as Q is increased. Right: λ_1/λ_2 (axial ratio) *vs.* Q for different lengths (N=6,7,..,17,18 from left to right). Axial ratio decreases drastically at $Q_c^L \simeq 4$. In both figures, values are for $T = 0.01$.

The most striking feature of Fig. 2 is that all the curves of R_g^2/N for different N values collapse on to the same curve. This curve describes a monotonously rising function – $f(Q)$. The PAs expand with the addition of any excess charge, but with a compact scaling. As Q increases the different curves break off, one by one, from this asymptotic function. This occurs when for each specific N it becomes "saturated" – the chain has reached its maximal extent.

The axial ratio decreases as Q is increased, which is consistent with expansion and elongation. However, as length increases, this elongation becomes less sharp: For the same Q longer chains have a higher axial ratio. This, again, indicates that when keeping Q constant the expansion is in a compact form – The configuration "inflates", but does

not elongate.

If we do not keep the excess charge constant but increase it as we increase the length of the chain, the size (radius of gyration) will grow "faster" that the compact scaling we have just described. Generally, if $Q \sim N^{\beta}$ then size will be $R_g \sim N^{\nu(\beta)}$. The interesting limit is when the scaling is "extended", that is $R_g \sim N$. Fig. 3 displays R_g/N as a function of $Q/N^{0.75}$. We see that the different curves for different lengths collapse on to the same curve. This curve describes a monotonously rising function $g(Q/N^{0.75})$. Repeating the same plot for different values of the exponent, we get a good collapse for the range $\beta = 0.7 - 0.8$. This means that R_g of chains of different lengths, for which $Q = xN^{0.75\pm0.05}$ will scale in an extended fashion with N.

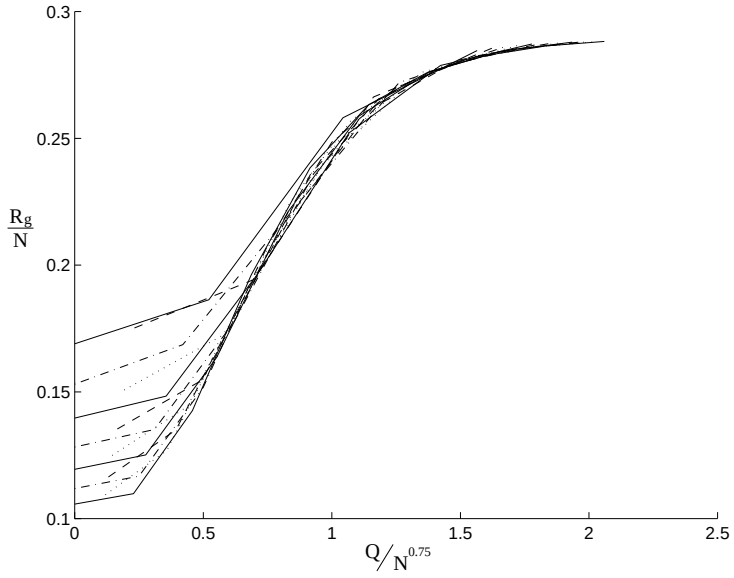

Figure 3: *R_g/N vs. $Q/N^{0.75}$* Curves are for different lengths (N=6,7,..,17,18 from top to bottom at the left). Note the collapse of the curves, "improving" as N increases. Data is for T=0.01.

To summarize we suggest the following conclusions:

1. For any excess charge $Q > 0$ the ground state expands from the most compact and dense configuration. In this sense, $Q_c^L = 0$.

2. For a given excess charge Q, R_g for PAs of different lengths scales in a compact fashion. That is:
$$\frac{R_g^2(N_1, Q)}{R_g^2(N_2, Q)} = \frac{N_1}{N_2} \Longleftrightarrow \frac{R_g^2}{N} = f(Q) \ , \tag{4.5}$$
provided $N > N_0(Q)$ above which the PA has not saturated yet.

3. For $Q \sim N^{0.75\pm0.05}$, R_g for PAs of different lengths has an extended scaling:

$$\frac{R_g(N_1, Q = xN_1^{0.75})}{R_g(N_2, Q = xN_2^{0.75})} = \frac{N_1}{N_2} \Longleftrightarrow \frac{R_g}{N} = g\left(\frac{Q}{q_0 N^{0.75}}\right) \ . \tag{4.6}$$

4. An increase of excess charge, for a given length, always increases R_g of the ground state – f and g are monotonously increasing functions.

Only for small (practically zero) excess charge there is a compact and dense ground state so Eq. 4.1 can describe the energy behavior. For larger excess charges, there is no condensation, the ground state is dilute and Eq. 4.1 does not apply.

4.1.2 Neutral Quenches – Energy Spectrum

We found that neutral quenches have a compact ground state. Now, we try to see if an extensive description applies well to describe their energy (Eq. 4.1). Apart from enabling a phenomenological description of the ground state energy, the extensiveness of energy in this model is of great importance. Should this not be the case or if the first order correction is not a surface term, all further discussions will be hampered. Many results for a finite system will not be applicable in the thermodynamic limit.

For all neutral, even-lengthed quenches of 6–18 monomers and partial samples for lengths of 18–26[5], all configurations were calculated and ground state energies were obtained.

Fig. 4 depicts the energy per monomer in the ground state for different chain lengths. For all neutral quenches of a certain length, the mean, maximal spread and the standard deviation of the ground state energy per monomer are specified. An extensive behavior means that as $N \to \infty$ we expect $E/N \to$ const. We chose the horizontal axis to be $1/\sqrt{N}$ – if the correction is indeed a surface term, E/N should be linear in such a scale. Viewing the graph, it seems that these are reasonable conclusions.

As discussed previously (section 2.2.3) the energy of a 2D salt crystal is extensive and bounds from below any other configuration of the neutral polymer. The energies obtained for a simulation of a salt-crystal are also displayed in Fig. 4. They can be seen to converge and fit rather well with an extensive description of the energy, $E = A_1 N + A_2\sqrt{N}$. They are also, evidently, a lower bound for all neutral quenches. We can, thus, set an extensive limit to the energy, but we would like our results for the quenches to support it.

For the quenched ensemble results are not quite as conclusive. Fitting the mean energy of the ensemble in an extensive, convergent form, results in:

$$\frac{E}{q_0^2} = (-0.133 \pm 0.005)N + (0.30 \pm 0.02)\sqrt{N} \ . \tag{4.7}$$

Should the energy diverge, we expect it to be a weak logarithmic divergence, owing to the nature of the interaction. We might try modeling it by $E = B_1 N \ln N + B_2 N$. We have applied this non-extensive form to our data with the result: $E/q_0^2 = (-0.042 \pm 0.002)N \ln N + (0.056 \pm 0.005)N$. Alas, over the range of N in our simulations (6–26) these two functions separate less than the errors of the results. We can not, therefore,

[5]For lengths 20, 22, 24 and 26 monomers we enumerated 1000, 500, 100 and 50 random neutral quenches respectively.

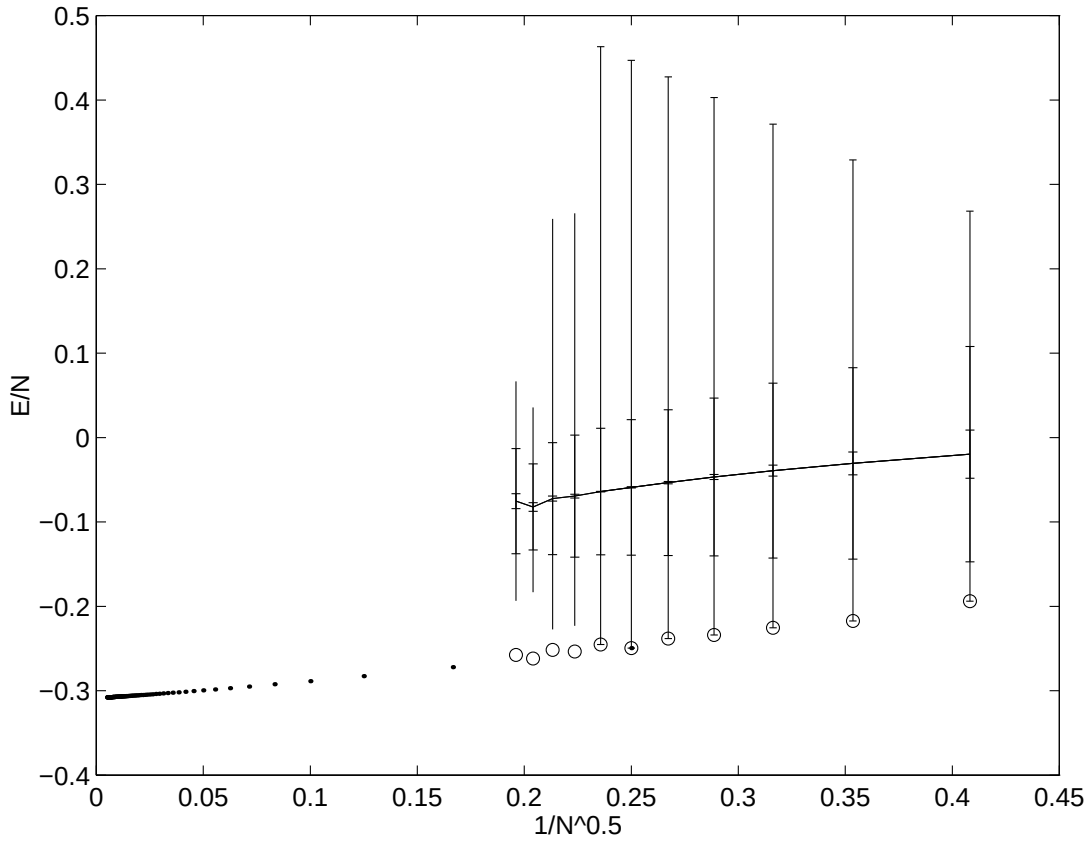

Figure 4: Ground state energy per monomer for sequences of lengths 6–26 monomers. Crosses on the error bars represent (going from the innermost outward): mean value (connected horizontally), statistical error of the mean, standard deviation and min/max values (for lengths 18–26, the error bar is not bounded, the min/max values are only of the partial ensemble of quenches taken, not global values). Results for the alternatingly charged quench are denoted by open circles. Simulation of a salt plane is denoted by dots. Horizontal axis is $\frac{1}{\sqrt{N}}$ to show linear behavior according to the expected scaling of energy.

distinguish between the two and assert the limiting behavior. We believe, though, that regarding the salt crystal as an extensive boundary is a valid assumption and the energy can be considered extensive.

Assuming a convergent form and plugging in the condensation energy obtained by Eq. 4.7, we try to find the correction to the bulk term in the energy. We fit our results to the form $E/q_0^2 = AN + BN^\beta$. For this we get $\beta = 0.50 \pm 0.02$. This is within the range expected for a surface correction term, but, again, this does not enable distinguishing between other possible logarithmic scalings (the surface correction may scale as $\sqrt{N}\ln N$ for example).

Naturally enough, the quench that assumes the lowest ground state energy is the one with alternating charges along the backbone, which was also studied separately (results

are also depicted in Fig. 4 and studied in section 4.4.1 below). It is the only quench that can create a configuration similar to the salt crystal which is the ground state of the 2D Coulomb gas, of which our polymers are a subset (see section 2.2.3).

The distribution of ground state energies within the ranges noted in Fig. 4 may be observed better in Fig. 5 where we display histograms showing the detailed distribution of the ground-state energy. We show these for chain lengths of 16, 18 and 20 monomers.

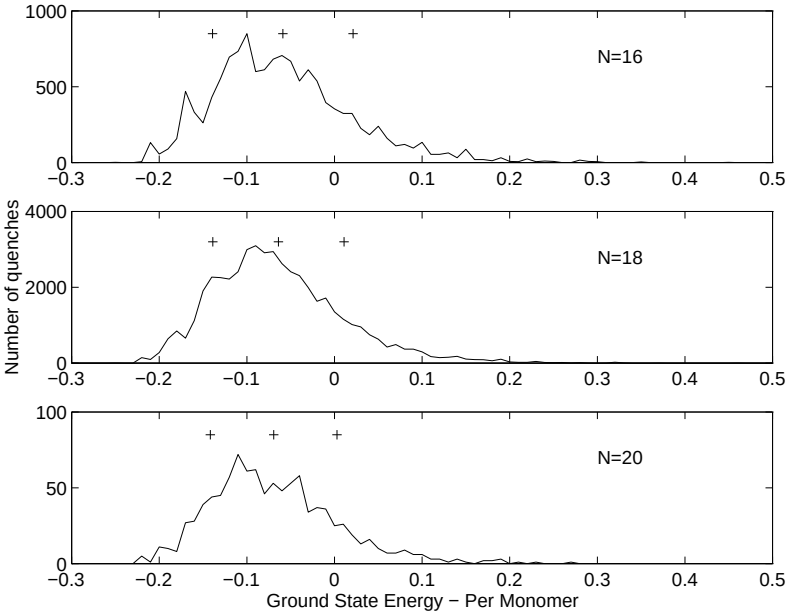

Figure 5: Distribution of ground state energy per monomer for all enumerated neutral quenches of lengths 16, 18 and 20 (only a partial sample of quenches for length 20). Crosses indicate location of mean and $\pm\sigma$ limits.

It is hard to tell from the histograms the type of the distribution and if it can be modeled in some form, especially since above 18 monomers the enumeration is partial. However an important feature we would like to check is if the ground state energy (per monomer) is a self-averaging quantity. This means that at the thermodynamic limit, a typical quench could be described by the average behavior. The extensiveness of the energy we have shown above is valid for the mean value, but does not necessarily represent the behavior of a randomly chosen quench – this will be true if the ensemble is self-averaging.

In Fig. 6 we plot the standard deviation of the ground state energy per monomer for the different lengths we studied (this is the standard deviation plotted previously in Fig. 4). Self-averaging requires that the standard deviation of the distribution, not only go to zero as the size of the system increases, but it must do so at a rate faster than $1/\sqrt{N}$. The

inset of Fig. 6 displays the same values plotted as a function of $1/\sqrt{N}$. We see that the behavior can be described very well as linear and reaching zero at the $N \to \infty$ limit. This implies that the ground state energy per monomer for the neutral PAs is a self-averaging quantity.

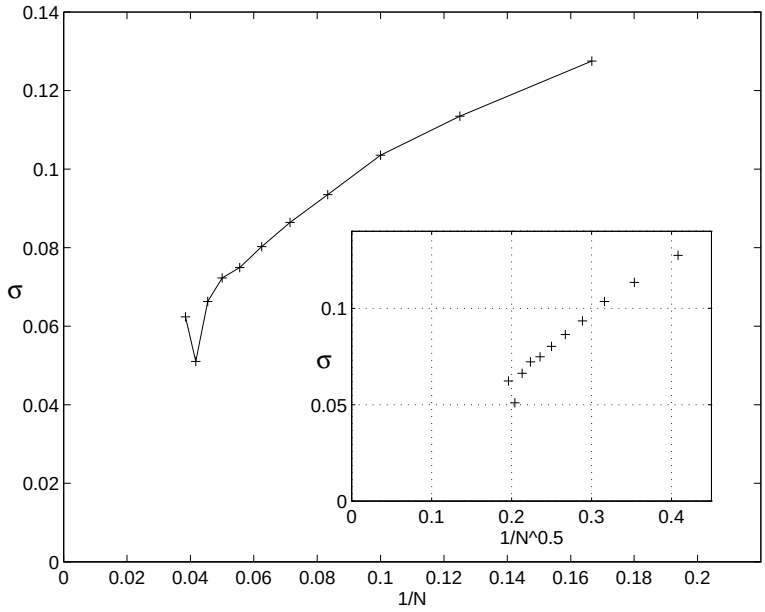

Figure 6: Standard deviation of the ground state energy per monomer – σ, as a function of $1/N$, where N, the chain length, is 6,8,...,26. Inset: The same standard deviation, but as a function of $1/\sqrt{N}$.

An important consequence of the self-averaging is that when joining together two neutral PAs of a certain length the energy of the new polymer is the sum of their separate energies (when discussing the configuration dependent contribution only, neglecting the different reference points of PAs of different lengths).

Although we argue the ground state energy is a self-averaging quantity, when averaging over all different quenches, charge sequence is an important parameter determining the behavior of the polymer. Later on we will see how this quench dependence manifests itself by influencing the type of collapse the chain undergoes and the possibility of a freezing transition.

4.1.3 Charged Quenches – Energy Spectrum

We now study the case when the chain has an excess charge $Q = q_0(N_+ - N_-)$. Thus far we have shown that a very small excess charge suffices for the electrostatic repulsion to dominate and the ground state will be extended. The energy cannot be modeled like a condensated drop as suggested by Eq. 4.1.

The ground state energies of all quenches and all possible excess charges are depicted in Fig. 7. We present the results for a length of 18 – it has the widest range of values for excess charge.

As seen in section 4.1.2 for neutral quenches, all quenches of the same excess charge have a large variance of the ground state energy. However, we can also see that the ground state spectrum reveals somewhat of a band structure with different bands corresponding to different excess charges. That is, the variance of the energies for a given excess charge does not exceed the separation between the different excess charges.

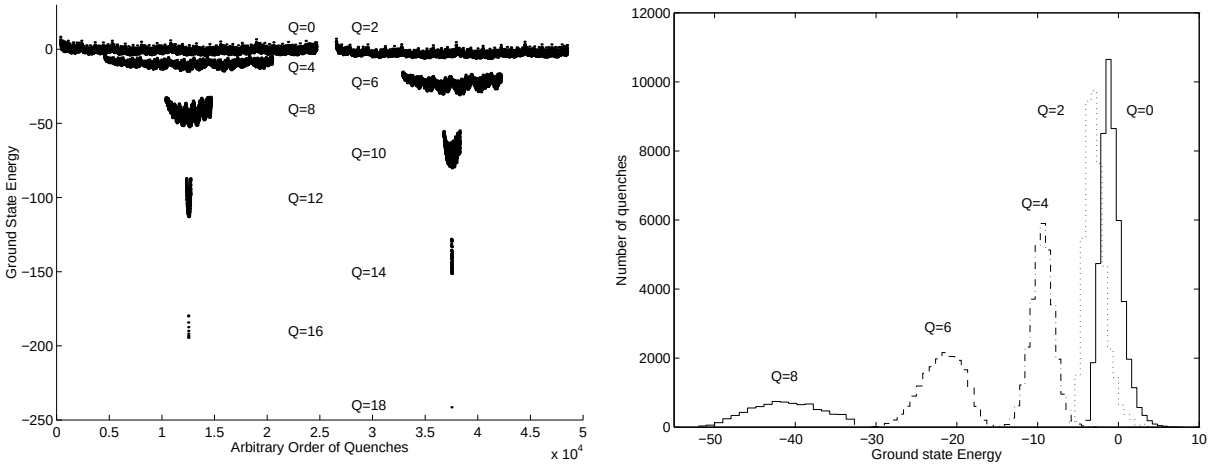

Figure 7: Left: The ground state energies of all quenches of 18 monomers. The abscissa's scale is an arbitrary order of quenches. Annotations denote the excess charge of the bands into which the energies group. Right: A histogram plot of the same energy distribution (only $Q = 0, 2, 4, 6, 8$ bands). Notice the overlap between the first few bands.

The band structure of Fig. 7 displays an irregular decrease of the energy with increasing excess charge. For a 3D system, similar plots [11] show an increase of the energy of the bands with increasing excess charge. This is quite natural as it requires some energy to charge the system. The energy displayed here is only the configuration-dependent contribution, as explained in section 2.2.2. It does not take into account the contribution of an excess charge dependent term, whose sign and magnitude depend on the arbitrary selection of the reference point. It can not be claimed that the energy of the quenches

with a higher excess charge have a lower overall energy than the less charged quenches.

The band structure is not definite. The histogram plot of the energy distribution in Fig. 7 displays an overlap of the least charged bands. The energy bands themselves do not have any apparent internal structure, as can be seen in the histograms for $Q = 0$ in Fig. 5, or if we focus on one of the band as seen in Fig. 8.

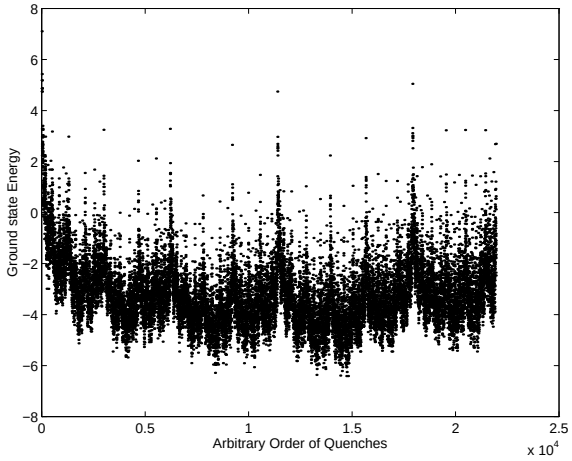

Figure 8: A closeup view into the structure of the $Q = 2$ energy band for an 18 monomer long chain. The abscissa's scale is an arbitrary order of quenches.

The appearance of a band structure indicates that the typical energy related to the excess charge is much more dominant than the fluctuations caused by charge sequence. This (and following the statements at the beginning of this section) lead us to roughly express the typical long-range part of the energy of the charged polymer as:

$$E(Q) \simeq -Q^2 \ln R \simeq -Q^2 \ln N \ , \tag{4.8}$$

where for an extended ground state, typical of most excess charges, the typical polymer size $R \simeq R_g \sim N$.

We expect the energy to scale linearly with Q^2 for a constant chain length – N. Fig. 9 shows the ground state energy as a function of excess charge, for the ensemble of 18-monomer long polymers. When scaled properly, displayed as a function of Q^2, the dependence of the energy is linear as expected. We can also see in Fig. 9 that this behavior breaks down for low excess charges: The fluctuations in the extensive condensation energy term dominate over the excess charge contribution and the above argument is not valid.

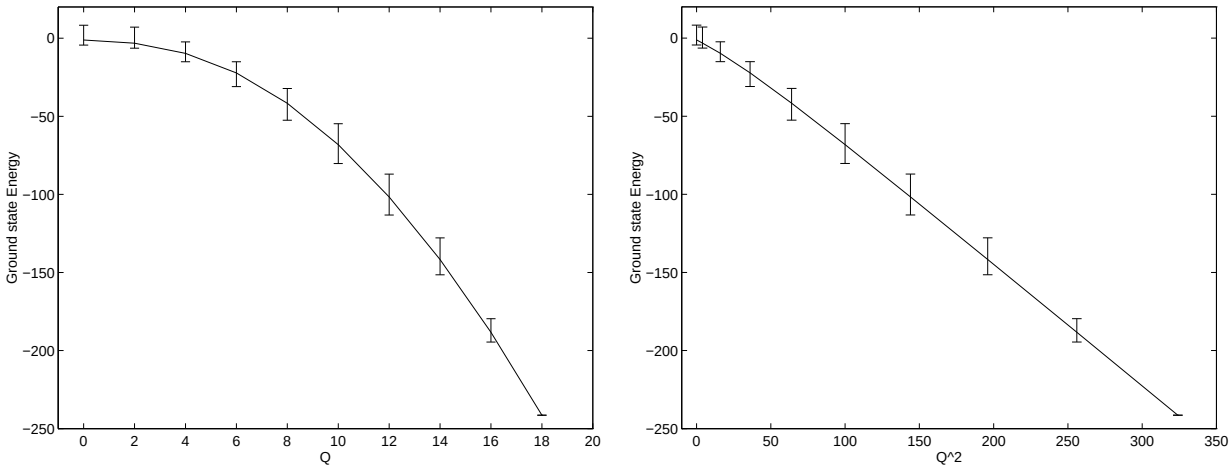

Figure 9: Left: $E_{g.s.}$ *vs.* Q. Right: $E_{g.s.}$ *vs.* Q^2, shows the expected scaling for the "more charged" quenches (Eq. 4.8). Error bars denote the full width of energy bands.

4.2 High-Temperature Properties

Opposed to the previously discussed low temperature properties of the system, we now study the other limit of very high temperatures.

At infinitely high temperatures the Coulomb interactions are irrelevant and the chain behaves like a SAW. Its spatial extent obeys: $R_g \sim N^{\nu}$, with $\nu = 0.75$ in two dimensions. Upon lowering the temperatures, the interactions start influencing the shape of the polymer. The volume of the PA may either expand or compress depending on the excess charge on it, the critical value being the high temperature critical charge – Q_c^H defined in section 2.1.5. This critical charge was calculated by Kantor and Kardar [22], whose derivation for a 2D system is as follows: At the infinite temperature limit the typical electrostatic energy of such a system is:

$$\overline{\langle U \rangle} \simeq -\sum_{\langle i,j \rangle} \overline{q_i q_j} \langle \ln |\mathbf{r_i} - \mathbf{r_j}| \rangle \simeq -\frac{1}{2}(Q^2 - q_0^2 N) \ln R_g \ , \tag{4.9}$$

where we assume a typical inter-particle separation on the order of R_g. $\langle ... \rangle$ and $\overline{\cdots}$ denote averages taken over all configurations and quenches respectively. It can be easily shown [22] that $\overline{q_i q_j} = (Q^2 - q_0^2 N)/(N^2 - N)$ for all pairs $i \neq j$.

We see that the interaction energy changes sign at $Q_c^H = q_0\sqrt{N}$, which we define as the high temperature critical charge. Excess charges above this value will cause the system to expand upon lowering the temperature, while excess charges below it will cause a contraction. In other words, for low enough excess charges there is an effective attraction between the fluctuations in the charge distribution. We can see that for a randomly charged chain the typical excess charge is the critical one and we need higher order expansion terms to determine the behavior. This result applies for all space dimensions.

This is only the lowest order approximation, describing only the first deviation from a SAW. This is the behavior at the high temperature end of the R_g *vs.* T curve (Fig. 1). This behavior is not expected to follow through, all the way down to zero temperature. For this reason we defined separately a low temperature excess charge. This also explains why the result given here does not comply with that of Ejtehadi and Rouhani [45] that estimate the critical charge to be $\sim N$.

Studying all chains of length 6–18, averaging over all quenches of the same length and excess charge, we examined the first deviation from the asymptotic value for R_g at high temperatures for all the R_g *vs.* T curves. We defined the critical charge by the

two values of excess charge between which the polymer changed its behavior (expansion and contraction). Figure 10 shows the different critical charges for all chain lengths enumerated. The charges are integer, so the relative errors are quite large. This and the limited lengths examined prevent the verification of the exact scaling law involved. However, the basic behavior, a slow growth of the critical charge with respect to N, is evident. Figure 10 also displays a $\sqrt{N}$ curve according to the theoretical prediction. We can see that it fits reasonably well the numerical results.

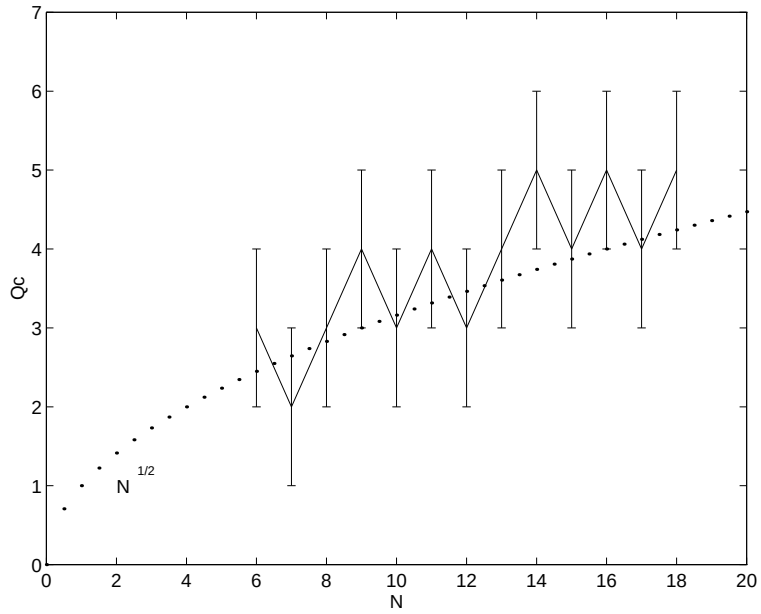

Figure 10: The high temperature critical charge (Q_c^H) for polymers of different lengths (N). Error bars are ± 1 in size, due to the integer charges and the parity of excess charge. The dotted line represents the theoretically expected $Q_c^H = q_0\sqrt{N}$ behavior.

Although we cannot assert the functional behavior of $Q_c^H(N)$, by comparing it to the results obtained for $Q_c^L(N)$, we can state that generally:

$$Q_c^H(N) \neq Q_c^L(N) \ . \tag{4.10}$$

It is important to acknowledge the existence of the two critical charges and their effect at the different limits. It seems to have been a source of confusion in some references.

4.3 Neutral Quenches – Transition Details

We now turn to the intermediate temperature regime to study the collapse from a SAW to a compact state as was described by Edwards *et al.* [16], and Higgs and Joanny [17] (see section 2.1.5). The collapse will occur only for quenches with an excess charge lower than the critical one. We investigate the features of the neutral quenched ensemble.

All neutral quenches of lengths of 6–18 monomers were studied over a temperature range of 0.01 to 10. As can be seen in Fig. 1 depicting the temperature dependence of R_g^2 for the 18 monomer long chain, on the average, the neutral quenches undergo a transition from an expanded random coil state at high temperatures to a compact one upon cooling.

The transition is "smooth" and does not have the characteristics of a phase transition. This can be seen when studying the temperature dependence of the heat capacity – Fig. 11. The graph shows the heat capacity *per degree of freedom* averaged over all neutral quenches for a given length (we take $2N-3$ degrees of freedom) for the range of temperatures studied. Previously, in section 4.1.2, we saw that the ground state energies (per monomer) converge and at low temperatures, as we see in Fig. 11, the curves seem to converge. At high temperatures the behavior is not obvious. We will argue that there is actually a logarithmic divergence with no limiting curve.

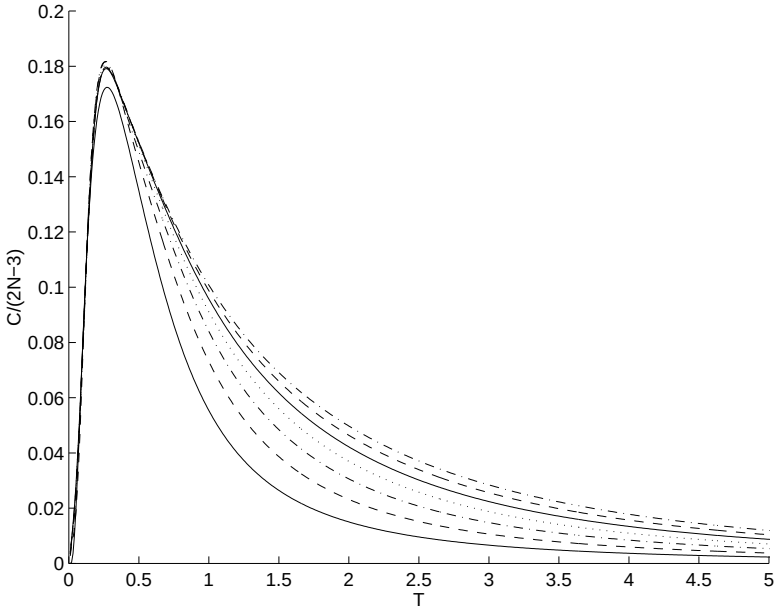

Figure 11: $C/(2N-3)$ *vs.* T for neutral quenches of different lengths: N=6, 8, 10, 12, 14, 16 and 18 from bottom to top.

The temperature of the peak in the heat capacity curve seems to be constant at

$T_0 \simeq 0.33 \pm 0.03$ and might seem to indicate a transition temperature. However, the neutral ensemble (as do the others) shows a very diverse behavior for different quenches. The average curves seen here are not representative of the typical curve of a single quench. For example, the average heat-capacity peak temperature for chains of length 18 is 0.34, but, with a standard deviation of 0.18. We discuss this diversity further when we deal with freezing (Sec. 4.6).

The heat-capacity peak can probably be attributed to the finite sizes we examine together with the discreteness of the lattice. It is possible that for a continuous system this feature will disappear and the heat capacity will reach its classical non-zero value at zero temperature. A finite discrete system, at low enough temperatures, will always become a two-level-model with the heat capacity dropping to zero, creating a peak at some intermediate temperature (Schottky anomaly [46]). The broadening of the peak for longer chains may be another indication that this is not a real transition, although we do not put it in quantitative terms.

The divergence of the curves in Fig. 11 and the non-extensiveness of the energy at high temperatures may be quantified by studying the area beneath the heat-capacity curve, which may be described as follows: The area is actually the difference in quench averaged energies at infinite and zero temperatures. At zero temperature the energy is that of the ground state which is lower bounded extensively (relying on previous discussions). At an infinite temperature all configurations have the same probability and averaging is simple algebraic. We can change the order of averaging, beginning with a single configuration, averaging over all quenches:

$$E_{\rm conf}^{\rm avg} = \overline{-\sum_{\{i,j\}} q_i q_j \ln r_{ij}} \tag{4.11}$$

$$= -\sum_{\{i,j\}} \overline{q_i q_j} \ln r_{ij} \tag{4.12}$$

$$= -\sum_{\{i,j\}} \left(-\frac{q_0^2}{N}\right) \ln r_{ij} = \frac{q_0^2}{N} \sum_{\{i,j\}} \ln r_{ij} \ . \tag{4.13}$$

We now average over all different configurations:

$$E^{\rm avg} = \left\langle \frac{q_0^2}{N} \sum_{\{i,j\}} \ln r_{ij} \right\rangle \simeq \frac{q_0^2}{N} \sum \ln \langle r_{ij} \rangle \ . \tag{4.14}$$

The last step can be justified by the behavior of the logarithmic function and the distri-

bution of R_g (see [2]). Assuming a scaling of $R_g \sim N^\nu$ we continue:

$$E^{\text{avg}} \sim \frac{1}{N} \cdot N^2 \ln N^\nu \sim N \ln N \ . \tag{4.15}$$

Since the heat capacity is divided by $(2N-3)$ degrees of freedom, we finally get that the area – A, is:

$$A = \frac{E^{\text{avg}}(T=\infty) - E(T=0)}{2N-3} \sim \ln N \ . \tag{4.16}$$

Figure 12 depicts the area beneath the C *vs.* T curves for different chain lengths. (The area is the theoretical value as defined above, not numeric integration.) It seems plausible that the calculated scaling is correct. By differentiating Eq. 4.16 with respect to N, we see that for large N, $\frac{dA}{dN}$ should scale linearly with respect to $\frac{1}{N}$. This can be seen in the inset to figure 12.

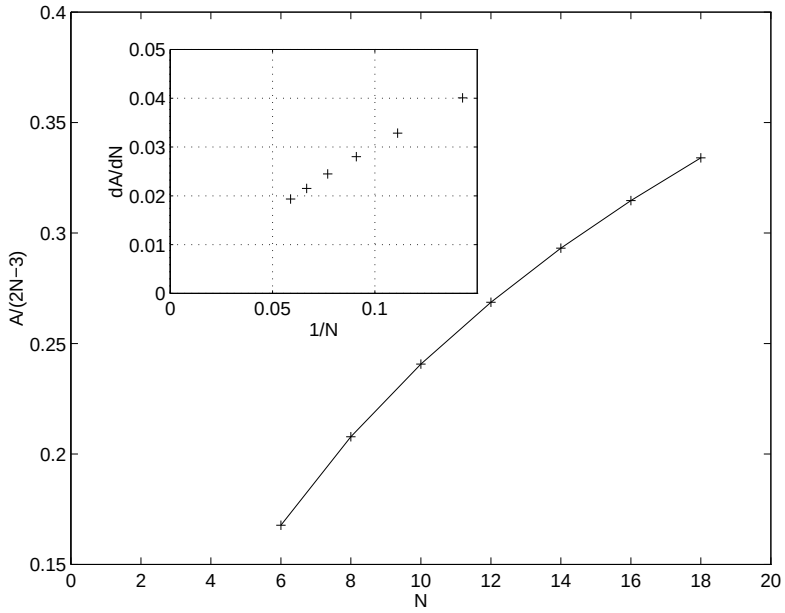

Figure 12: Area (A) *vs.* N. Inset: dA/dN *vs.* $1/N$, an attempt to linearize the graph under the assumed scaling. In both cases area is divided by $(2N-3)$ degrees of freedom.

Generally, for an extensive system we would expect this area to be constant. The results indicate this is not the case here. There is a continuous crossover between different temperature regimes in which different effects dominate. This is a result of the long-range interaction, unlike, as described earlier, short-range interacting systems that undergo the Θ-transition. Kantor and Kardar [15] show that, for a random sequence of charges, above four dimensions the Coulomb interaction ceases to be a relevant parameter and we might expect a Θ-transition.

4.4 Specific Quenches – Transition Details

In several cases earlier we have stated the importance of charge sequence in determining the polymer's behavior. We now focus our attention on two specific quenches: The alternating charge sequence, which, as it turns out, has a some interesting properties not common to other neutral quenches. We also study the homogeneously charged polymer, that as the extreme case of excess charge exhibits interesting behavior as well.

4.4.1 Alternating Charge Quench

Victor and Imbert [19] claimed that an alternating charge quench (+ − + − ...) is significantly different from other neutral ones. Its collapsed globular state does not create a screened phase of a "liquid" nature as proposed by Edwards *et al.* [16], and Higgs and Joanny [17]. Rather a dielectric, dense phase should appear. In this case its behavior should follow that of short-range interacting systems, with an effective attraction. We should, therefore, observe the regular Θ-transition.

To check this claim, the neutral alternating charge sequences of lengths 6–26 monomers were studied separately from the general neutral ensemble. The results we present here do not contradict Victor and Imbert's claim. However, the short lengths involved here prevent confirmation of an actual phase transition.

The critical temperature we found (identified as the peak in the heat capacity curve, Fig. 13 below) is $T_c = 0.16 \pm 0.01$. This is similar to the result in [19]: $T_c \simeq 0.1$. However, this relatively low temperature is very near the freezing to the ground state, a region that in our case displays some irregular, discretization dependent behavior and should, therefore, be regarded with caution.

We do not observe a divergence in the height of the heat capacity peak at the critical temperature as we increase the chain's length. However, the area beneath the curve, per degree of freedom, displayed in Fig. 14, seems to remain constant for different chain lengths. This is consistent with a possible phase transition.

If we assume that there is indeed such a phase transition we would expect a scaling behavior of the following form as we approach the peak temperature T_c:

$$\left\langle R_g^2(N, T_c(N)) \right\rangle \sim N^{2\nu_c} \ . \tag{4.17}$$

We were not able to perform a finite size scaling analysis for the lengths we examined, however, should this be the case we expect all $\left\langle R_g^2(N) \right\rangle / N^{2\nu_c} vs.\ T$ curves to intersect at

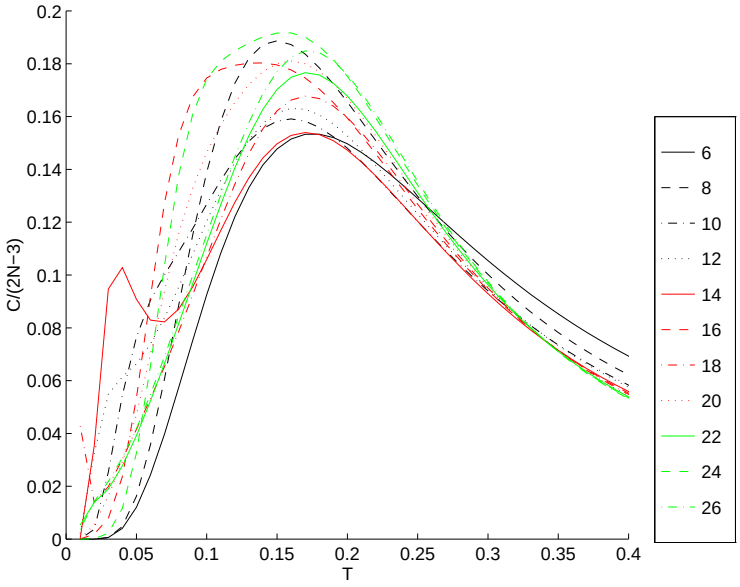

Figure 13: C (per degree of freedom) *vs.* T, for alternating charge sequences of lengths 6,8,...,26.

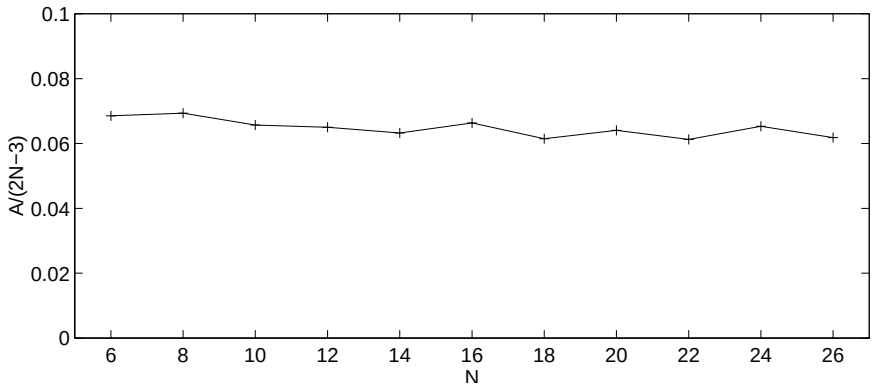

Figure 14: Area beneath heat capacity curve *vs.* N. The area is normalized to $(2N-3)$ degrees of freedom.

the critical temperature. Victor and Imbert [19] find $\nu_c = 0.59 \pm 0.01$. Various authors [44] studied short-range interacting homopolymers with results in the range $\nu_c^{SR} = 0.5 - 0.6$. Golding and Kantor [44] find for a short-range interacting heteropolymer $\nu_c = 0.60 \pm 0.02$.

Fig. 15 shows these curves for different values of ν. We can see that almost all curves coincide at the critical temperature of the heat capacity ($\simeq 0.16$) for $2\nu \simeq 1.1 - 1.2$, similar to the short-range interaction critical exponent.

The top graph in Fig. 15 demonstrates an interesting zero temperature peculiarity. The ground state is not the most compact – R_g^2 increases a bit when approaching zero temperature. The system prefers a configuration that can be divided up into aligned

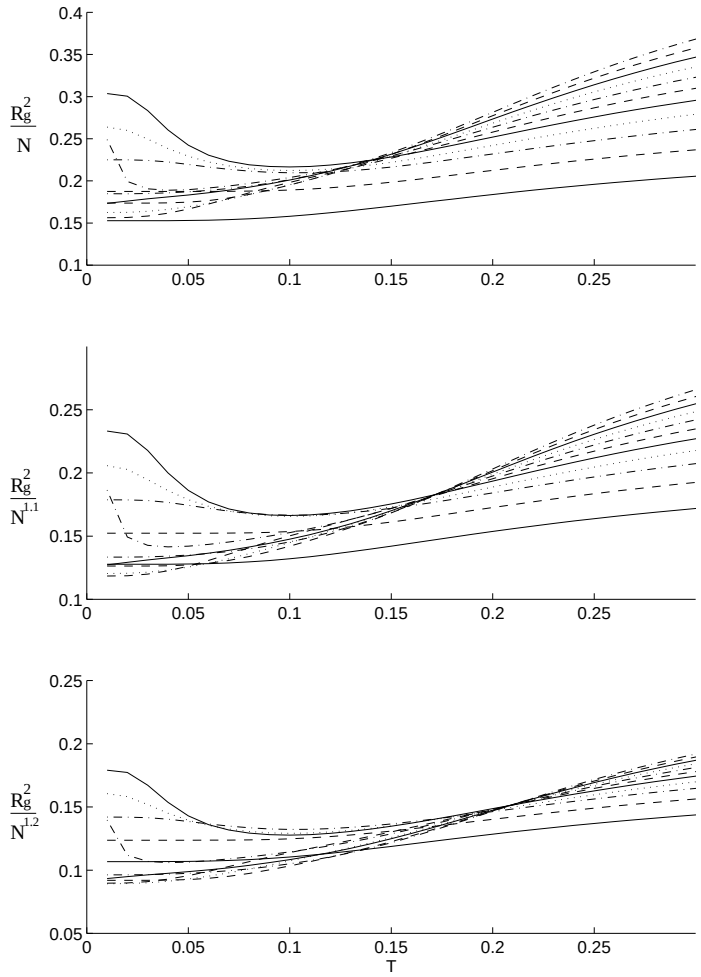

Figure 15: $R_g^2/N^{2\nu}$ *vs.* T for different ν and N. N is 6,8,..,26 running from bottom to top at the high temperature end in every subplot.

dipoles so interactions die out much faster. It seems that as a result of the long-range interaction, for the finite and rather small systems studied, the surface tension becomes relatively negligible. A local perturbation, unpaired charges or non aligned dipoles, has a great effect on the energy. A chain of 16 monomers can fold to an exact square shape making it, naturally, the most favorable. A chain of 18 monomers, on the other hand, prefers a 9×2 rectangular array configuration over the more compact 6×3 rectangular array configuration. This is displayed graphically is section 4.5, discussing the annealed ensemble. When comparing all possible *compact, rectangular* configurations for longer chains, it seems this irregularity dies out and the most compact is energetically favorable.

4.4.2 The Fully Charged Quench

Another interesting case is the fully charged quench. All monomers are positive (or negative) so they all repel each other. This is of special interest as an extreme case of the system we study. It is also similar to that of polyelectrolytes where all charges have the same sign, a model that has been subject to extensive study.

Unlike the neutral quenches, in this case the ground state is the fully extended, rod-like configuration. Higher energy configurations allow contraction into less extended states.

We will now argue that in this case for all finite temperatures only the ground state exists, all higher energy excitation states are forbidden. The lowest excitation above the ground state would be that of a single "stair" like step (Fig. 16).

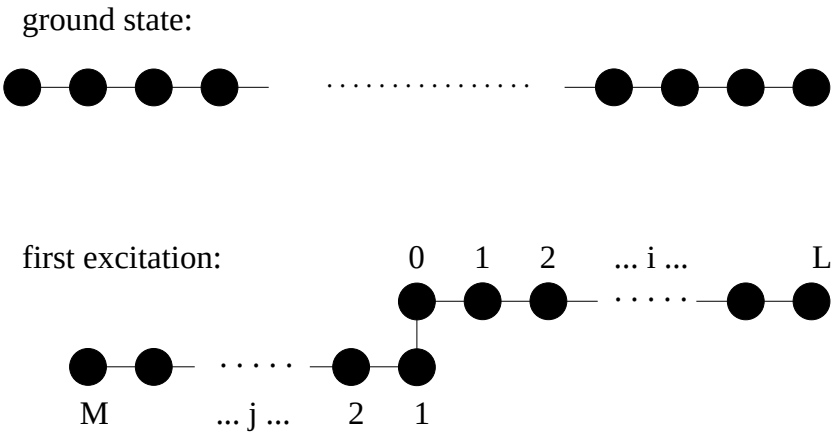

Figure 16: Ground state and first excitation of a positive only chain of length $N = L + M + 1$.

We now estimate the energy required for such an excitation. The change in energy of the charge i relative to the ground state is:

$$\frac{\Delta E_i}{q_0^2} = \sum_{j=1}^{M} \left[-\ln \sqrt{(j+i-1)^2+1} - (-\ln(j+i)) \right] \tag{4.18}$$

$$= \sum_{j=1}^{M} \left\{ -\frac{1}{2} \ln \left[(j+i)^2 \left(1 - \frac{2}{j+i} + \frac{2}{(j+i)^2} \right) \right] + \ln(j+i) \right\} \tag{4.19}$$

$$= -\frac{1}{2} \sum_{j=1}^{M} \ln \left[1 - \frac{2}{j+i} + \frac{2}{(j+i)^2} \right] \tag{4.20}$$

$$= \sum_{j=1}^{M} \left[\frac{1}{j+i} + \mathcal{O}\left(\frac{1}{(j+i)^3} \right) \right] = \sum_{j=1}^{M} \frac{1}{j+i} + \mathcal{O}(1) \ . \tag{4.21}$$

The sum can be calculated by integration using the Euler-Maclaurin formula [47], where

the highest order correction is still $\mathcal{O}(1)$.

$$\frac{\Delta E}{q_0^2} = \sum_{i=0}^{L} \frac{\Delta E_i}{q_0^2} = \sum_{i=1}^{M} \left[\ln\left(M+i+1\right) - \ln\left(i+1\right) + \mathcal{O}(1) \right] \ . \tag{4.22}$$

Again, using the Euler-Maclaurin formula, this results in:

$$\begin{aligned} \tfrac{\Delta E}{q_0^2} = (L+M+2)\ln(L+M+2) \ &- \ (M+1)\ln(M+1) \\ &- \ (L+2)\ln(L+2) + \mathcal{O}(N) \ . \end{aligned} \tag{4.23}$$

We define α as the fraction of the chain on one side of the bend: $N = L+M+1$; $M = \alpha N$; $L+1 = (1-\alpha)N$. Inserting these relations into the expression above, we get:

$$\frac{\Delta E}{q_0^2} = \alpha N \ln\left(\frac{N-\alpha N+1}{1+\alpha N}\right) - (N+1)\ln\left(1-\frac{\alpha N}{N+1}\right) + \mathcal{O}(N) \ . \tag{4.24}$$

We see that the energy associated with the lowest possible excitation scales as N. (For a finite number of configurations, when the "stair" is near the edges, the change in energy scales as $\ln N$.) On the other hand, there are $\sim N$ such possible excitations (wherever we choose to make the "step" within the chain), so the entropy scales as $\ln N$.

If we examine the free energy $F = U - TS$, we see that in the thermodynamic limit, at every finite temperature, energy considerations always win over the entropic ones. This means that *the system will always remain in its ground state with no transitions to other, less extended, states.*

We enumerated all configurations for this quench of lengths 6–26 monomers. Our simulations, exhibit a divergence of the "transition temperature" (defined as the peak in the heat capacity) with respect to N. This is consistent with an absence of any transition at the thermodynamic limit. Fig. 17 depicts the heat capacity of the chain at different temperatures for various lengths. The divergence of the transition temperature is evident. An interesting phenomenon is the dying-out of the peak, possibly another indication of the disappearance of excitations at the thermodynamic limit.

Although we claim that there is no transition, we attempt to quantify the behavior of the peak in the heat capacity curve for our finite system. At high temperatures, the behavior of the chain is that of a SAW, with a characteristic separation between charges of $R_g \sim N^{\nu_{SAW}}$. The characteristic energy of such a state, with respect to the ground state will then be:

$$\Delta E \sim -N^2 \ln R_g - E_{gs} \sim N^2 \ln N \ , \tag{4.25}$$

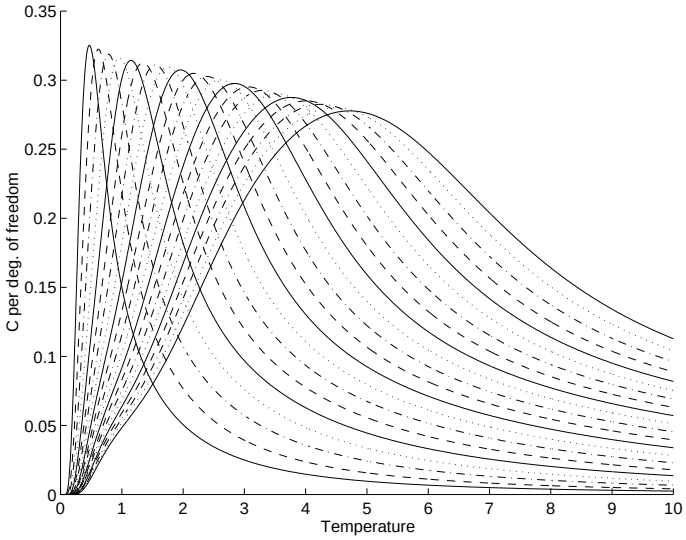

Figure 17: C *vs.* T. Results for polymers of lengths 6–26 charges are displayed, with the peaks moving to higher temperatures and lowering down for longer lengths. It must be remembered that the transition here is to an expanded state (not a collapse).

where the energy of the ground state E_{gs} also scales as $-N^2 \ln N$ but with a larger prefactor because the typical distance is larger. The crossover will occur when the thermal energy of all modes will be on this scale:

$$N^2 \ln N \sim N k_B T_c \Rightarrow T_c \sim N \ln N \ . \tag{4.26}$$

Fig. 18 displays T_c, the heat capacity peak temperature, for the different lengths examined. Fig. 18 also shows an attempt to linearize the graph according to the expected scaling behavior (we manipulated the axes to bring the dependence of Eq. 4.26 to a linear form for large N). Results in this case can be seen to be inconclusive.

We attempted to fit the T_c *vs.* N curve (Fig.18) to a functional form of $T_c = AN^{\alpha}$. For the whole graph this results in $\alpha = 1.55$. The interesting procedure, though, is to apply this form to consecutive, overlapping, 9-point segments of the graph, in search of the limiting behavior for the exponent. Results, presented in Fig. 19, show this exponent for different parts of the curve in Fig. 18.

We see that, as chain length (N) increases, the exponent α decreases towards 1. This could indeed be an indication of an $N \ln N$ dependence (which is actually N to a power slightly larger than one).

The question remains if this transition is a feature of a real continuous system or a lattice discreteness effect. The fact that the peak dies out as N increases may indicate that it is a lattice effect. For long enough chains, the short-ranged lattice step may become

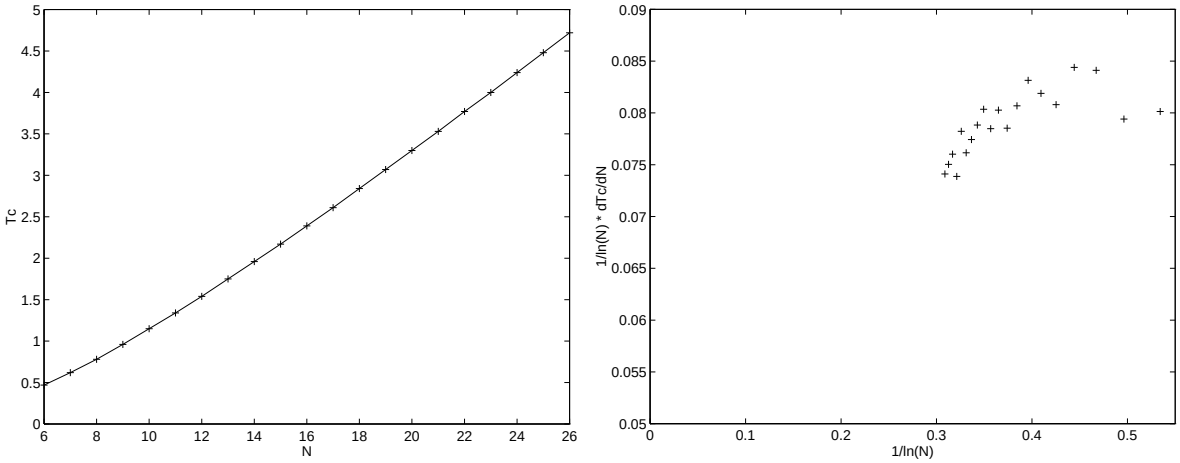

Figure 18: Left: T_c *vs.* N. Right: $1/\ln(N) * dT_c/dN$ *vs.* 1/ln(N). An attempt to linearize the graph under the scaling assumption.

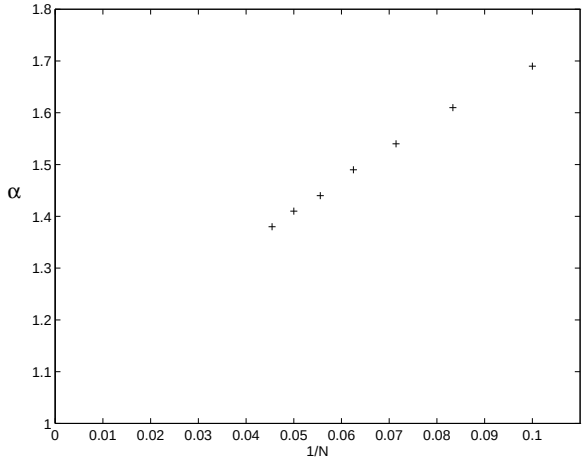

Figure 19: The scaling exponent α of T_c for different 9-point segments of Fig. 18. Each segment is represented by its middle value of N.

irrelevant. For a continuous system there will be a continuous spectrum of excitations. The reasoning we applied concerning the discrete lattice will not hold and we might observe a different behavior of the heat capacity.

4.5 The Annealed Ensemble

In the annealed ensemble charges are free to move along the backbone, with a restriction on the total excess charge. Only a single charge may occupy each monomer. At zero temperature, they naturally fall into the sequence and configuration that have the lowest possible energy.

We searched for the ground state of every sequence with all different lengths of 6–18 monomers and all possible excess charges. The charge sequence with the lowest ground state energy was selected. The ground states for each annealed ensemble are shown in Figs. 20, 21, 22 for chain lengths of 16, 17 and 18 monomers respectively.

For the lowest possible excess charge (0 for even lengths, 1 for odd), the selected sequence is the alternating charge sequence, which has a compact ground state. This is expected since this ordering of charges allows a ground state most similar to the salt-crystal configuration, which we have identified earlier as the global lower bound for this system. All other excess charges ($Q > 1$) have a fully extended, rod-like shaped, ground state. Hence, $Q_c^L = 0, q_0$ (for even/odd lengths).

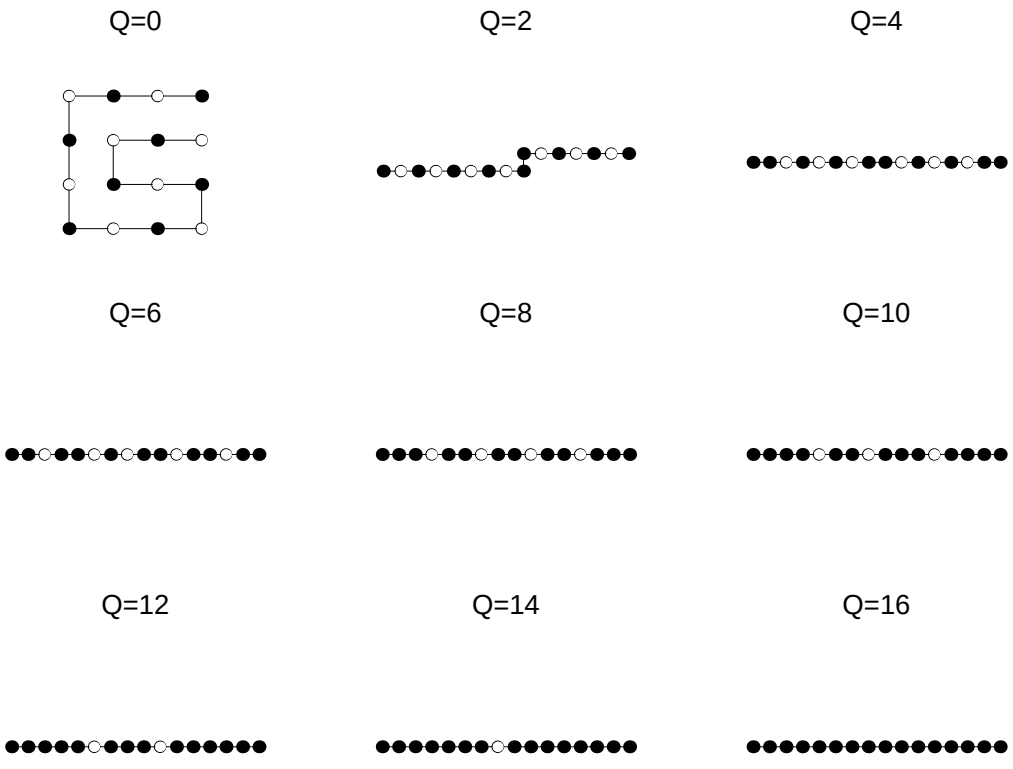

Figure 20: Ground state configurations for annealed sequences of length 16, with an overall excess charge Q.

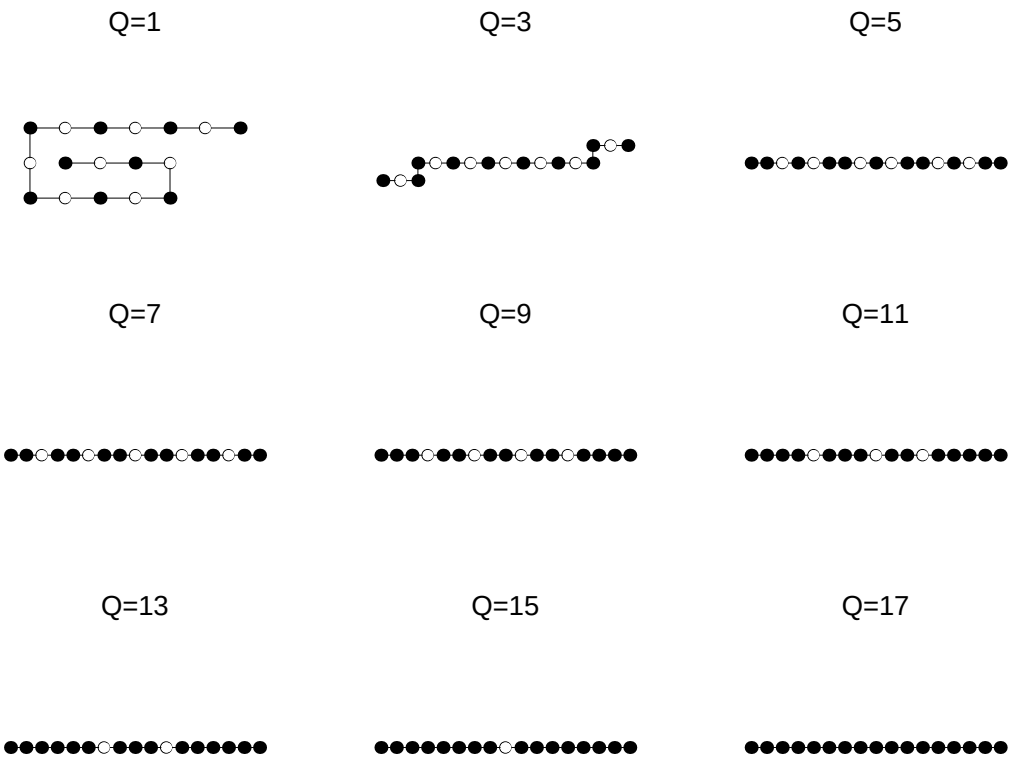

Figure 21: Ground state configurations for annealed sequences of length 17, with an overall excess charge Q.

The ground state of the neutral, 18 monomer long chain displays an interesting peculiarity. The sensitivity to the charge is such that an elongated but symmetric shape is preferred over a more compact one. We saw similar behavior when studying the alternating sequence, which is the same case. This is probably a result of the limited length – for longer, neutral chains a compact ground state is energetically favorable.

The finite lengths examined do not exhibit a definite behavior of the charge sequence the ground state realizes. If we consider the excess charge as being distributed on a finite neutral rod, then a simple calculation shows that being evenly spaced along the rod is energetically favorable over concentrating half of the excess charge at each edge of the rod. This does not prove the optimal distribution of the charge which we believe will tend to be constant along the rod, with an increase in density near the edges.

For a 3D system it has been speculated by Kantor and Kardar [22, 23] that for annealed PAs, with high enough excess charge, the ground state should be a compact, neutral shape with a "finger" carrying the excess charge protruding away from it. We can see here that for two dimensions the behavior is quite differen. The long-range effects of the logarithmic

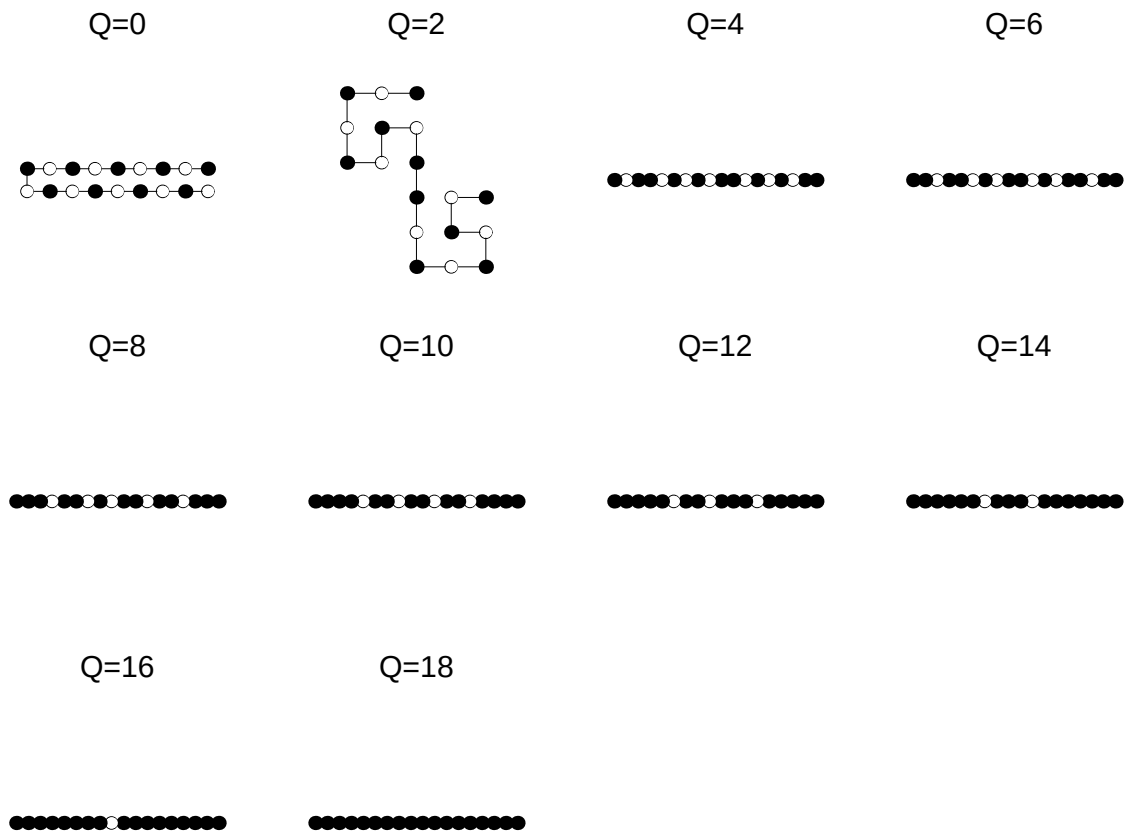

Figure 22: Ground state configurations for annealed sequences of length 18, with an overall excess charge Q.

Coulomb interaction are so pronounced that any minute deviation from neutrality will cause an effective global repulsion and expansion of the polymer. This is in agreement with the theoretical predictions we made in section 4.1.1, when discussing the Rayleigh drop model. The numerical results for the critical charge of the quenched ensemble have shown that $Q_c^L = 0$ but a highly extended ground state appears only if the excess charge grows like: $Q \sim N^{0.75}$. The annealed ensemble is much more sensitive, maximally expanding for a minimal excess charge.

A word of caution must be entered to this discussion: As stated by Kantor and Kardar [11], the effects of lattice discreteness are much more pronounced for annealed PAs. Contrary to the quenched ensemble, where the ground state is averaged over many quenches, thus smoothing out lattice effects, the annealed ensemble's ground state corresponds to a single configuration of a single sequence. The chains studied might not be long enough to overcome this problem.

4.6 Investigation of Freezing

Thus far we did not consider the exact nature of the transition to the low energy states. In all previous sections we calculated exact thermodynamic values describing the system. These values are relevant and present a good description of the system's behavior if it is in thermal equilibrium. One result of such an assumption is that the system will minimize its free energy at all temperatures and will be found in its global energy minimum configuration at zero temperature.

However, for this type of system we may not rule out the possibility that it exhibits a freezing transition. As discussed in section 2.1.6, disordered systems that tend to be frustrated might, upon cooling, get caught in a local energy minima state – not the global one. The probability of escaping and finding the ground state may be, depending on the features of energy landscape, exceptionally small. The system will remain in this meta-stable state, violating the minimization of the free energy principle. Such a transition could be attributed to the degree of disorder in the system and independence of states.

One straight-forward way to check for the appearance of such a transition is to repeatedly evolve a system in time and check if it relaxes into different states of different energies each time it is cooled down (simulated annealing). We will adopt a different approach – studying thermodynamic aspects of the system that may be indicative of such a transition. The specific observables we study are defined to point out properties of the system that are considered as inducing freezing. These observables have been defined for the study of different systems such as spin glasses or short-range interacting polymers. Here we apply them to our system.

The previous results have shown that only neutral quenches have compact ground states. It is likely that freezing will occur in a compact shape, where drastic maneuvers of the polymer between different states are restricted and the energy gradient is larger. We studied 20 random neutral quenches, 18 monomers long. The results, as we will present, indicate the absence of a freezing transition. One of the most apparent features (although not rigorously examined) is that many properties of this ensemble seem to be non-self-averaging. Different quenches show a great diversity in their behavior.

Results will be presented as follows: We will explain the different measures taken in search of freezing. For each, we will display the results for 4 representative quenches, designated (a)–(d) in figures 23, 24, 25 and 26 and draw the conclusions regarding freezing.

At the same time we will see how the differences between the different quenches manifest themselves in the different parameters studied.

A natural starting point is to consider the heat capacity. We do not expect a divergence of the heat capacity for this transition, but, irregular features of the curve at low temperatures may point toward some phenomenon. Moreover, the freezing transition is related to a drastic reduction in the number of states – the entropy crisis, the heat capacity which is a measure of energy fluctuations may express this.

Figure 23 displays the heat capacity (C) of the four representative quenches as a function of temperature. For each, there is a maximum at a certain temperature, but the peaks are each of a very different nature: The peak temperature and the slopes of the curves when approaching it vary widely. We do not see any feature that may imply a phase transition.

In section 4.3 we saw that there is a peak in the heat capacity curve that is possibly a lattice effect or a result of the normal compactifying of a neutral polymer to the globular state. We will, therefore, also look at another parameter that may be also important:

As stated earlier, a freezing transition is characterized by a drastic reduction in the number of states thermodynamically accessible to the system. A measure for this number of states is given by the parameter:

$$X = 1 - \sum_{k=1}^{\text{conf}} p_k^2 \ , \tag{4.27}$$

where $p_k = (1/Z)e^{-E_k/k_B T}$ – the canonical probability for a certain configuration.

It can be seen that at high enough temperatures, when all states have the same probability $X \to 1$. The deviation from the asymptotic value will behave as $X \simeq 1 - 1/S$, where S is the number of states. On the other hand, nearing zero temperature, only one configuration will dominate: $X \to 0$[6].

In a system following the REM definition, X should change linearly between the two limiting values, when averaged over all quenches (or all realizations of disorder, in general) between the temperatures 0–T_f, where T_f is the freezing temperature [32].

In figure 23 we display the X parameter on the same temperature scale as the heat capacity. We expect a rise in X to occur together with the heat capacity peak. Indeed,

[6] In our model, reflection symmetry causes each non-rod state to be counted twice. For this reason X goes to a lower limit of 0.5 instead of zero. Since the two states are degenerate this still represents a single ground state.

this is roughly the behavior. Quenches (b) and (c) exhibit an interesting feature. The heat capacity shows a "hump" or a minor peak when rising. The "transition" in X occurs at that temperature, of the minor peak. We might interpret this in the following manner: Upon lowering the temperature, there is a first transition from a SAW to a collapsed dilute globular state. This transition manifests itself only in the heat capacity because there is still a large number of states accessible to the system. At a lower temperature there is a second collapse or, maybe, freezing which is pronounced in the minor peak in the heat capacity and the rapid decrease in X.

There is another feature we should note: We can see that X drops off towards 0.5 (equivalent to zero in the theoretical definition) at low temperatures. However, only for quenches (a) and (b) it actually reaches 0.5. That is, at finite temperatures, there is only one dominant configuration – the ground state. For the other two, even at low temperatures $X \neq 0.5$, meaning there are a few (2-3) thermodynamically relevant configurations – "more" indicative of a possible glass phase.

We now try to understand the nature of these suspected transitions. Freezing, described by REM as resulting from an entropy crisis at low temperatures, depends on the sharp decrease in the density of states at low energies. We examine the low energy tail of the energy distribution for the different quenches in Fig. 24. We see the distribution of the 100 lowest energy configurations. Again the different quenches display a varying spectrum. Generally the distribution falls off at lower energies but at different rates. A freezing transition would be indicated by a few near low energy states.

We can see that for quenches (a) and (b) there is one isolated ground state. Hence, there is a good chance the system will relax to the global minimum energy configuration. These are also the two quenches for which X dropped to zero in Fig. 23 which is consistent with the definition of X. The other two quenches, (c) and (d), have a few near low energy states (they even seem to be have some degeneracy, though actually they don't). They would be more likely to undergo a freezing transition, should it occur. The probability of occupying one of the low energy states is not negligible compared to the ground states even at low temperatures. This is not enough to prove freezing, it remains to be seen that the transition from the low energy states to the ground state is "difficult", otherwise, they will gradually fold into it.

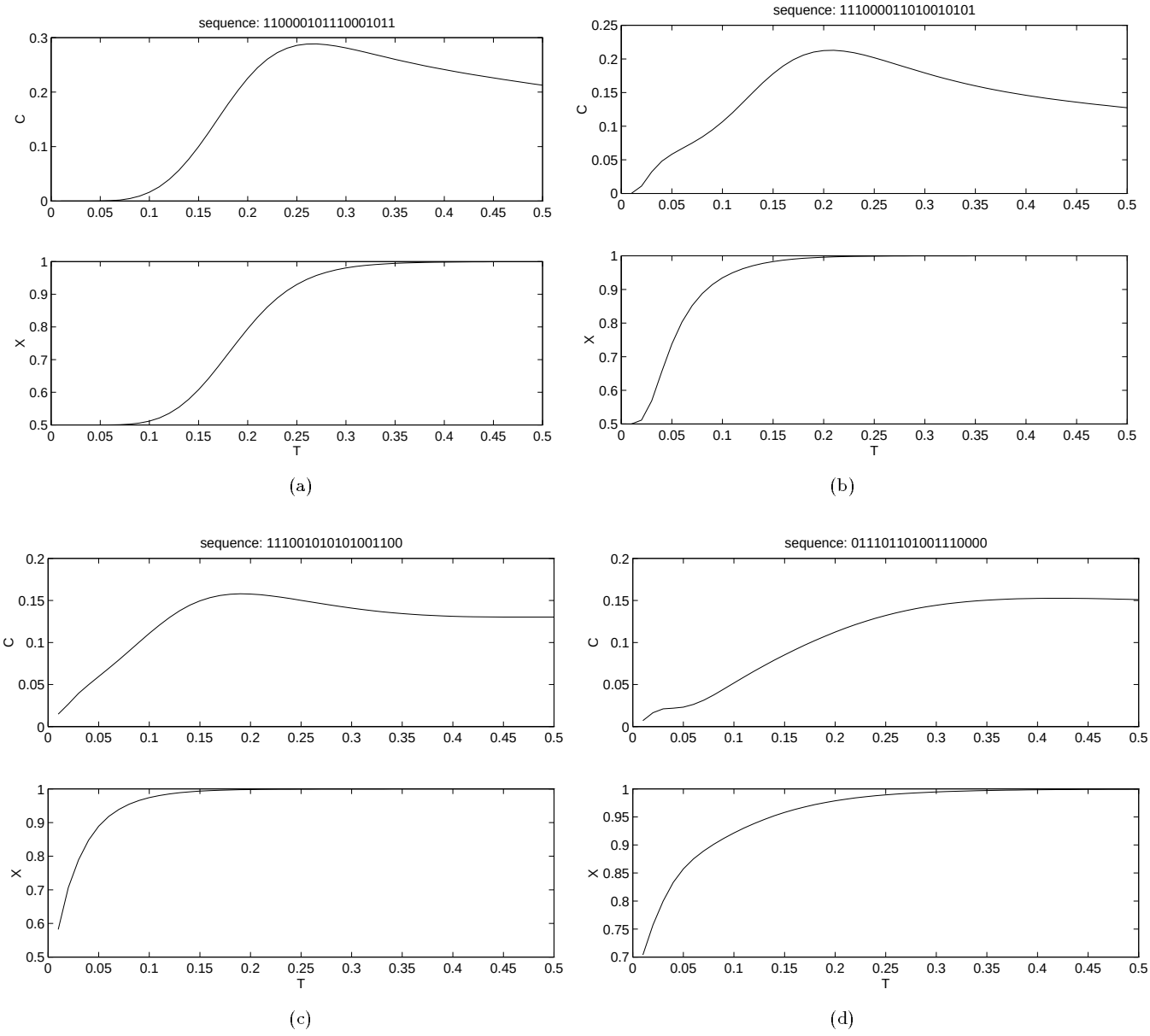

Figure 23: Four different neutral charge sequences. For each C *vs.* T (top) and X *vs.* T (bottom) are displayed on the same temperature scale. (a)-(d) are four different quenches appearing also in the following graphs. '1'/'0' in sequence denote +/- charges.

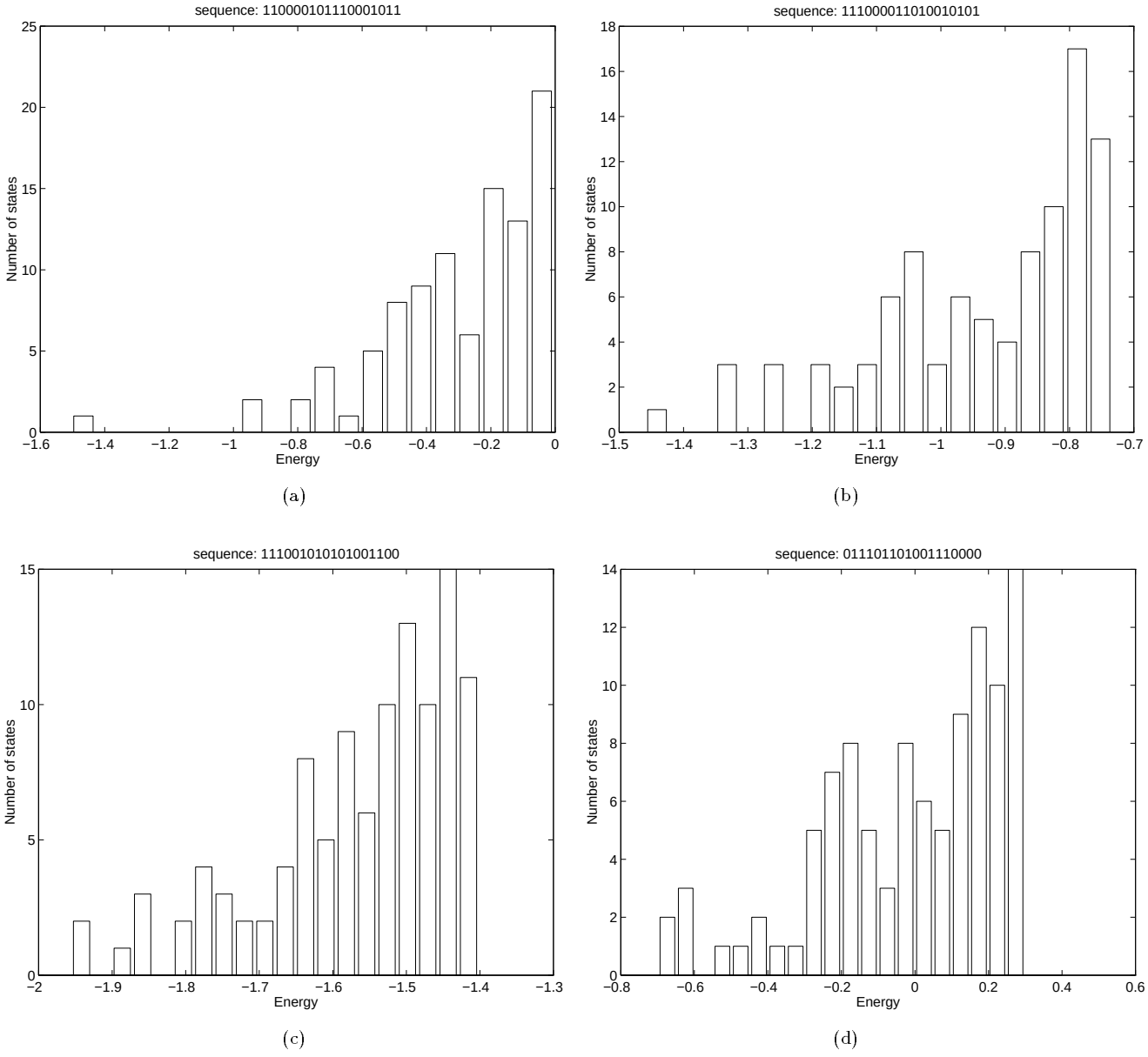

Figure 24: Distribution of the 100 lowest energy configurations for four different neutral charge sequences. Sequence notations follow figure 23.

We would now like to see if these low energy states are distant in the "configuration-energy landscape". For freezing to occur they must be "distant" so transition between them will be less likely – more barriers to overcome. In Fig. 25 we draw the configurations of the 9 lowest energy states, for each of the four quenches. Careful observation reveals that the different configurations have many similar elements, in some cases they are almost identical. This may imply that there is no freezing transition. The similarity of states allows easy relaxation to the real ground state at low temperatures and the system does not freeze into meta-stable states.

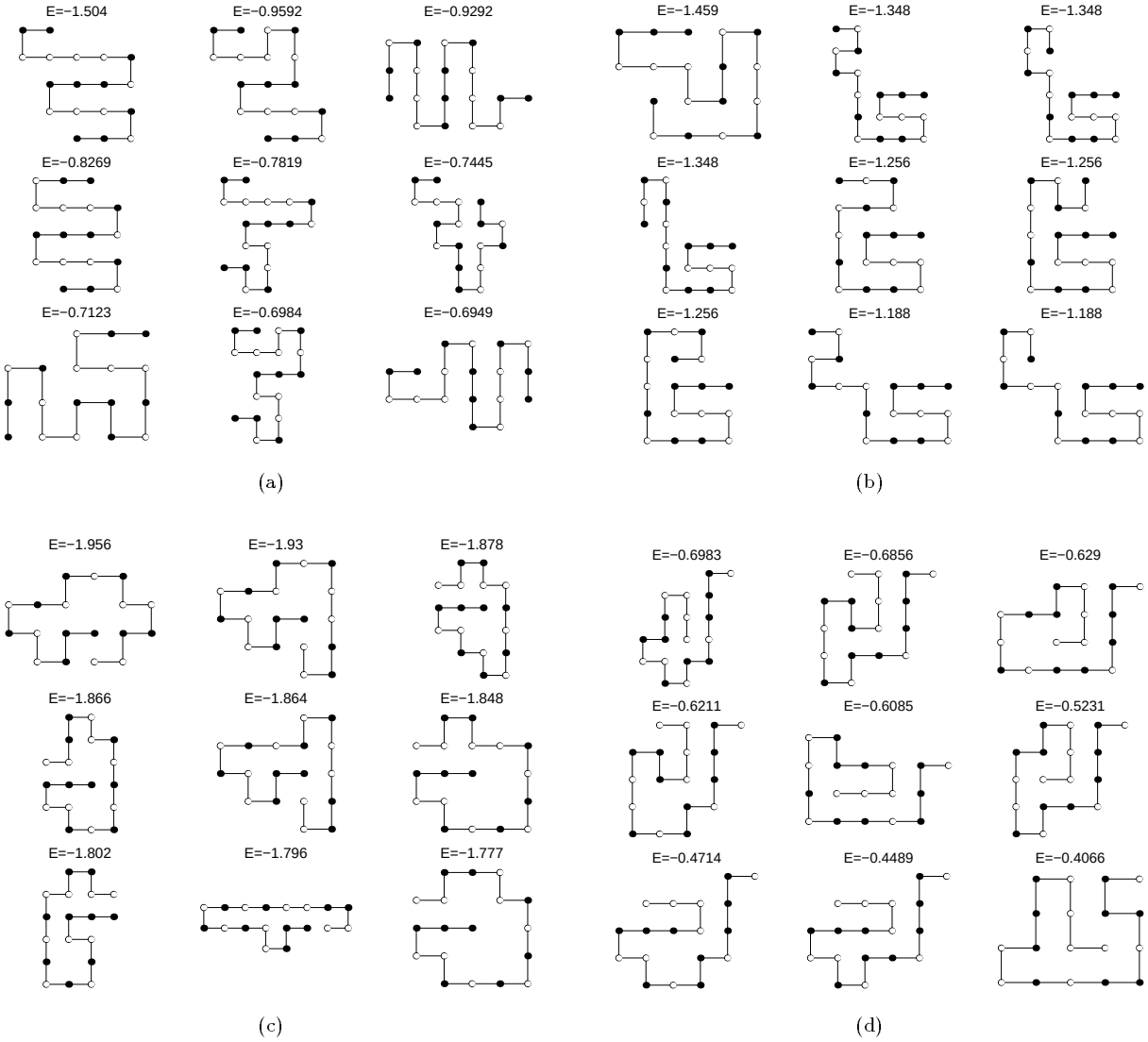

Figure 25: Paths of the 9 lowest energy configurations for the same four different neutral quenches as in the previous figures.

The previous "visual" argument is now put in more quantitative terms. One would expect two different states in the glass phase to have similar energies, but to be structurally different. A local minima configuration will have a low probability of relaxing to the global minimum if they are distant in the configuration space. For short-range interactions, this "distance" is measured by the number of common contacts in the 2 configurations. Because each contact contributes to the energy, this also is a measure of how much the energies are similar and also measures structural similarity. (For normalization, the ratio to the maximum number of possible common contacts is taken.) Such a measure, which can be considered as the overlap of the two states, will range between 0 (different states) and 1 (similar).

PA systems with long-range interactions require a more complex treatment. In this case different structural changes have different energy costs (in the short-range case they were the same). This must be taken into account when measuring "distance" between states. Pande *et al.*[35] who have studied the freezing transition for PAs, suggest a modification of the short-range parameter for the long-range interaction. For every pair of two configurations: α and β, we define $Q_{\alpha\beta}$[7] as:

$$Q_{\alpha\beta} = \sum_{i \neq j} f(\mathbf{r}_i^\alpha - \mathbf{r}_j^\alpha) f(\mathbf{r}_i^\beta - \mathbf{r}_j^\beta) \ , \tag{4.28}$$

where $\mathbf{r}_i^\alpha$ is the position of the i'th monomer in configuration α. $f(\mathbf{r})$ is the dependence of the interaction on distance. For the Coulomb potential:

$$f^{d\neq 2}(\mathbf{r}) = \frac{1}{|\mathbf{r}|^{d-2}} \ ; \ f^{d=2}(\mathbf{r}) = \ln \frac{|\mathbf{r}|}{r_0} \ . \tag{4.29}$$

$Q_{\alpha\beta}$ is divided by $max[Q_{\alpha\alpha}, Q_{\beta\beta}]$, so it will range between 0 (distant configurations) and 1 (similar configurations). The $Q_{\alpha\beta}$ parameter is also directly connected to the statistical dependence of states [35]: Large $Q_{\alpha\beta}$ values point towards a high correlation between the states, thus violating the REM assumption.

Following Shakhnovich *et al.*[29], we observe the similarity (or overlap) only between the relevant states at every temperature. Each pair of states $\langle\alpha\beta\rangle$ is assigned a probability which is the product of their separate Boltzmann factors.:

$$P_{\alpha\beta}(T) = \frac{e^{-(E_\alpha + E_\beta)/k_B T}}{\left(\sum_\alpha e^{-E_\alpha/k_B T}\right)^2} \ . \tag{4.30}$$

[7] This is not to be confused with excess charge, which is zero throughout this section.

The distribution of the $Q_{\alpha\beta}$ parameter is studied with respect to this probability, in the following fashion:

$$P(Q_{\alpha\beta}, T) = \sum_{\alpha'\beta'} P_{\alpha'\beta'}(T)\delta(Q_{\alpha'\beta'} - Q_{\alpha\beta}) \ , \tag{4.31}$$

where we sum over all configuration pairs. This means we find which configuration-pairs contribute to each value of $Q_{\alpha\beta}$, each pair with its respective probability.

If a system freezes to a glassy phase we would expect to have some pairs of states with a mutual $Q_{\alpha\beta}$ that tends to zero (meaning they are different). Their probabilities are expected to be significant at low temperatures, so the distribution of $Q_{\alpha\beta}$ will be dominated by these pairs.

For different temperatures we calculated the distribution function of $Q_{\alpha\beta}$ as displayed in Fig. 26. Due to the complexity of this calculation, we limited ourselves to the 100 lowest energy conformations of each quench. This is justified when studying figures 23-25 and seeing they are the only relevant states.

We can see that at very low temperatures only the ground state is relevant. Obviously, the ground state is similar to itself so we get $Q_{\alpha\beta} = 1$. As temperature is increased more states become thermodynamically relevant. However, they are all similar, as expressed by their high mutual $Q_{\alpha\beta}$ values that appear in the histogram. Even at the infinite temperature limit, when all states have the same probability, all of them are similar, no $Q_{\alpha\beta} < 0.5$ is obtained[8]. This is to say that all the low energy configurations are "close" one to the other in configuration space and the chances of being trapped are low.

The quenches we previously suspected as having a freezing transition, (c) and (d), do indeed have relatively low $Q_{\alpha\beta}$ values at low temperatures, but even these are high enough to reflect a similarity, or high correlation of states. For a short-range interacting system (or other systems exhibiting freezing in the REM sense) this distribution tends to be peaked near zero when approaching the thermodynamic limit.

All of the different criteria we studied seem to point towards the absence of a freezing transition. Even when there are some low energy states (as opposed to a single isolated one) they have similar configurations. The system will not freeze into one of several meta-stable states but will always be able to find the real energy minima – it will not become a glass.

[8]This is not the real infinite temperature limit, since we consider only the lowest 100 states, but we assign them equal probabilities.

It would only be fair to state that the conclusions must be regarded with caution. We are dealing with the low temperature behavior of the system. In this region, especially when the lengths involved are relatively short, the model's discreteness plays a great role. The apparent energy gap between the low energy states (Fig. 24) will probably decrease in a continuous system.

It can also be seen that some quenches have a "tendency" to a glass – their properties are nearer to it than others. Making the chains longer may enhance their behavior in this direction. We see that in the presence of long-range interactions, the specific sequence of monomers is of great importance. The alternating sequence, for instance, has a large ground state degeneracy unlike the sequences displayed here. Maybe the natural selection of amino acid sequences, allowing their "correct" folding, is affected by this feature as well.

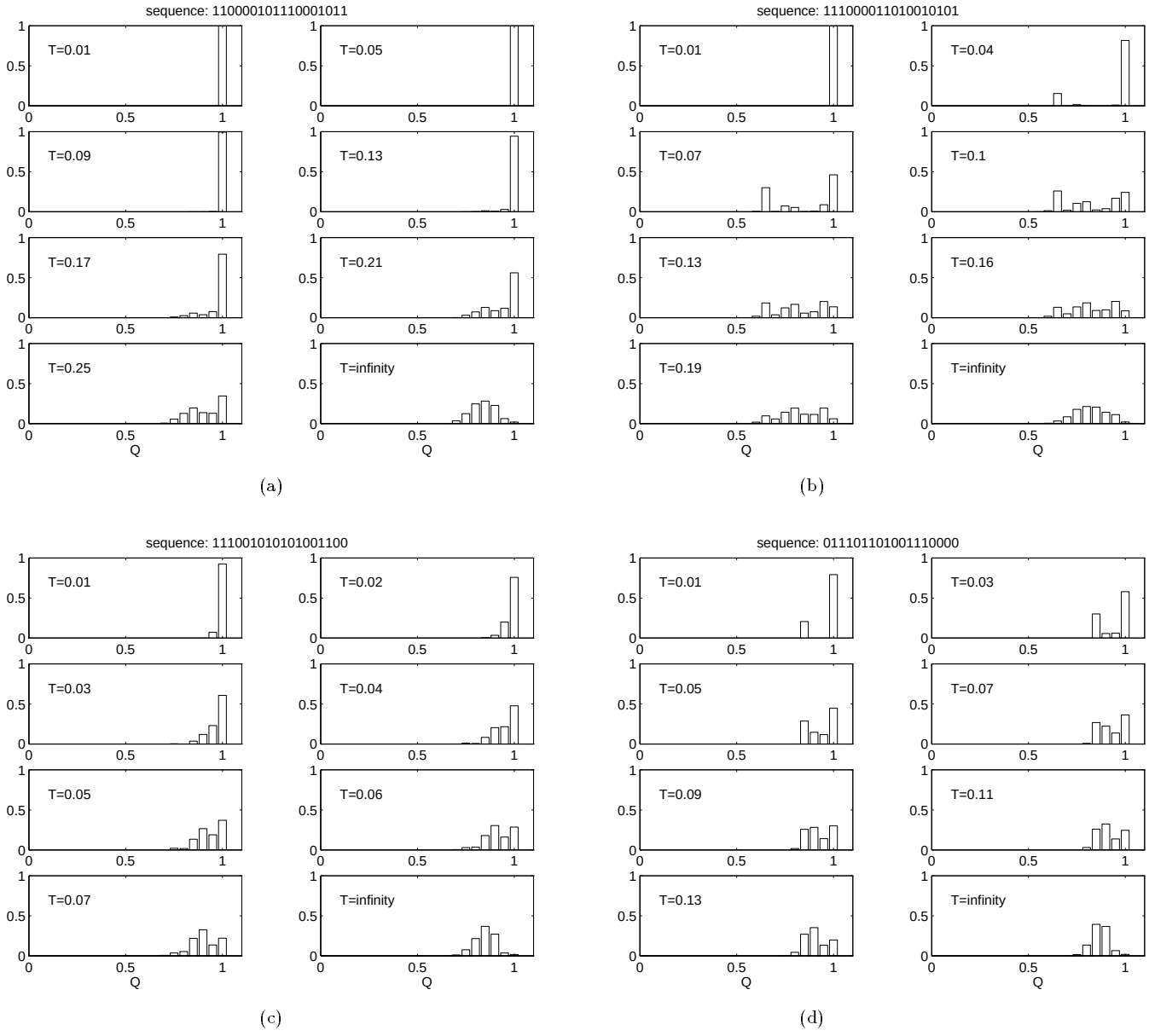

Figure 26: The distribution of $Q_{\alpha\beta}$ at different temperatures for four different neutral quenches. $\alpha\beta$ are all pairings of the 100 lowest energy states. Sequence notations follow figure 23.

5 Conclusions

We studied the properties of a polymer with positive and negative charges along its backbone – a polyampholyte. The study was of a 2-dimensional lattice model, mainly using numeric methods (enumeration) along with some analytic estimations. The properties investigated were of energetic (energy spectrum, heat capacity) and conformational (spatial extent, shape transition) nature.

The logarithmic 2-dimensional Coulomb potential turned out to be a key factor in the system's behavior. Many basic features, such as convergence of energy had to be given special attention. This must be taken into account when trying to apply our results to higher dimensions, especially since one of the main motivations for this model was a better understanding of phenomena encountered in similar models for three dimensions.

We find that the neutral polyampholytes collapse from their high temperature random behavior to compact states with an extensive energy in their ground state. This collapse does not display the characteristics of a phase transition. It appears that only strict neutrality allows collapse into a compact dense shape. The long-range potential makes the system very "vulnerable" to any excess charge – on the average, any excess charge will cause the system to relax to an expanded state.

Several properties of the quenched ensembles seem to be non-self-averaging and charge sequence plays a major role in their behavior. An extreme case of the alternating charge seems to behave like a short-range interacting polymer, featuring the Θ-transition. Others differ vastly in their "transition temperature", energy landscape and radius of gyration at different temperatures.

The investigation the possibility of a freezing transition is not conclusive, but it seems the system does not undergo such a transition. The low energy states are highly correlated, thus violating REM.

Many phenomena we encounter, especially at low temperatures, are suspected as lattice discreteness effects. This may also be true for real polymer systems, but certainly requires further study of longer chains or analytic continuous models.

The complexity of the enumeration method is such that major improvement of computer speed is needed to increase the lengths studied significantly. Understanding the low temperature behavior of this system requires some rigorous analytic study.

A Energy of a Two-Dimensional Salt Crystal

We present the full derivation of the energy of a finite 2-dimensional salt crystal: An overall neutral configuration of positive and negative charges of equal magnitude, q_0, on a 2D square lattice. The charges occupy the nodes in an alternating sign order – "checkerboard" configuration.

The general question, the stability of a many charge system, has been addressed previously in several articles (for example [48]), but the results do not apply to potentials of the logarithmic type we encounter here. The proof we provide here is restricted only to a very specific configuration of such charges.

We are interested in the type of energy function, that is we would like to show it is extensive with the first order corrections being a surface term:

$$E = -\epsilon_c V + \gamma S = \left(A_1 N + A_2 \sqrt{N}\right) q_0^2 \ , \tag{A.1}$$

where in a 2D system $V \sim N$ and $S \sim \sqrt{N}$. We do not calculate the values for the condensation energy – ϵ_c, or the surface tension – γ, but prove their existence. For clarity, we drop the q_0^2 factor in the rest of this section.

The basic problems this derivation deals with are the divergence of the logarithmic interaction and the mathematical complexity of summing up the discrete contributions. The general scheme we apply is to divide the plane into small, repeating, neutral subunits whose interaction is then much weaker (multipole-multipole) and falls of fast enough with distance. At large distances we are able to integrate over a continuous spread of such units enabling the overall calculation.

For a finite system we will have to take into account finite size and discretization corrections. The total energy can be considered as a sum of the idealized configuration with several contributions, or corrections. We will deal separately with each of them in the following sections.

Condensation energy for an infinite plane

We choose to divide the plane into be "quadrupole" units (Fig. 27), for the reasons stated above. We calculate the energy of a quadrupole, at the coordinate center, interacting with all others. If the total interaction, for the infinite plane converges, then there is a finite condensation energy (neglecting surface effects).

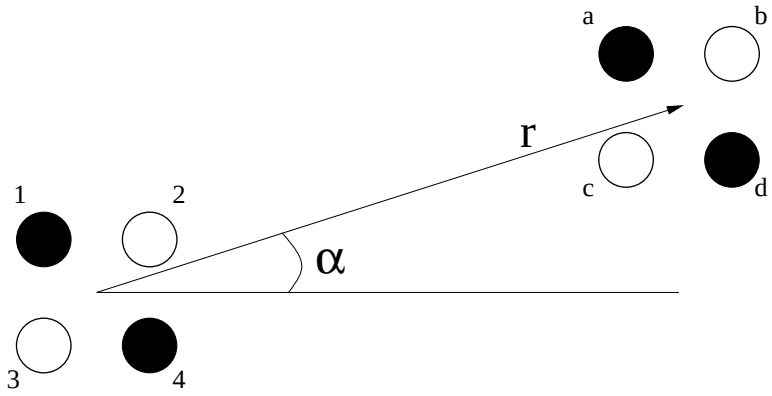

Figure 27: Two interacting quadrupoles in a plane.

We now calculate the quadrupole pair energy, where one is centered at $(0,0)$ and the other at (r,α) (Fig. 27). We find it more convenient to perform the calculations in complex coordinates where $z = r\cos\alpha + i\sin\alpha$ and $E = \ln|z| = \Re(\ln z)$ (for clarity, we omit the $\Re$ notation below). The energy is comprised of 16 pair interactions:

$$\begin{array}{ll} E_{1a} = E_{2b} = E_{3c} = E_{4d} = -\ln z & \\ E_{1b} = E_{3d} = \ln(z+1) & E_{1c} = E_{2d} = \ln(z-i) \\ E_{2a} = E_{4c} = \ln(z-1) & E_{3a} = E_{4b} = \ln(z+i) \\ E_{1d} = -\ln(z+1-i) & E_{2c} = -\ln(z-1-i) \\ E_{3b} = -\ln(z+1+i) & E_{4a} = -\ln(z-1+i)\ . \end{array} \tag{A.2}$$

Summing up all the above contributions and extracting $\ln z$ from all parts, the pair energy is:

$$\begin{array}{rl} E^{qq} = & 2\ln\left(1+\frac{1}{z}\right) + 2\ln\left(1+\frac{i}{z}\right) + 2\ln\left(1-\frac{1}{z}\right) + 2\ln\left(1-\frac{i}{z}\right) \\ & + \ln\left(1+\frac{1+i}{z}\right) + \ln\left(1+\frac{1-i}{z}\right) + \ln\left(1-\frac{1+i}{z}\right) + \ln\left(1-\frac{1-i}{z}\right) \quad . \end{array} \tag{A.3}$$

Allowing for a constant energy term of interaction with quadrupoles up to a distance $|z_0| = r_0 \gg 1$, we calculate the correction, the interaction with quadrupoles beyond this region. We approximate $\ln(1+z) \simeq z - z^2/2 + z^3/3 - z^4/4$. All terms relating to the first three orders cancel out. We remain with:

$$E^{qq} \simeq \Re\left(-\frac{6}{z^4}\right) = \Re\left(-\frac{6e^{-4i\Theta}}{R^4}\right) = -\frac{6\cos 4\Theta}{R^4}\ . \tag{A.4}$$

At these large distances the quadrupole surface density can be considered constant. We can then integrate over the whole plane, (r,α) ; $r > r_0$. This integral converges with the angular integration going to zero. Of course, all higher order terms will converge as well. We conclude that for an infinite plane of the 2D salt crystal the energy per charge is has a finite constant limit.

Correction for surface quadrupoles

In a finite plane, quadrupoles close to the boundaries don't see the same surroundings as in the infinite plane that was calculated above. When the plane is large enough we can locally approximate the surface boundary to be a straight line. Thus, the difference in energy between a quadrupole near the surface and that of one in the center is the interaction with the "missing outside half-plane" – Fig. 28. This correction should be added up for all charges on the line normal to the surface, leading inward. Its convergence means a constant energy correction for every surface element, thus ensuring a total correction proportional to the surface size.

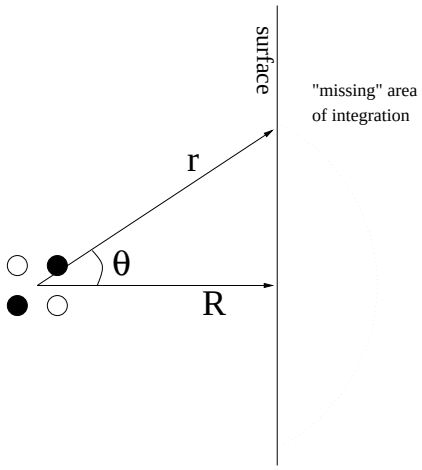

Figure 28: The configuration for the calculation of the surface energy.

The interaction energy of a quadrupole at a distance R from the surface with the "missing" half plane is:

$$\begin{aligned} E^q_{surf}(R) &= \int_R^\infty \int_{-\theta}^{\theta} E^{qq}(r,\alpha) d\alpha \; r dr \\ &\simeq \int_R^\infty \int_{-\theta}^{\theta} \frac{6}{r^4} \cos(4\alpha) d\alpha \; r dr \; , \end{aligned} \tag{A.5}$$

where $\cos\Theta = \frac{R}{r}$. Again, we neglect a constant surface contribution at short distances and find the correction at large distances. The angular integration will at most be between $(-\pi, \pi)$ (depending on r) so it can be bounded by some finite constant. The radial integration converges as well, so:

$$|E^q_{surf}(R)| < \frac{\text{Const}}{R^2} \; . \tag{A.6}$$

Integration of this correction (as a function of R) from the surface inward converges, thus, insuring a finite surface energy correction from each surface element. The result is that the total contribution of this correction will then grow as the size of the surface.

Interaction of single charges on the boundary with the bulk

The residual charges on the surface must also be accounted for. Due to the shape of the finite plane, not all charges necessarily group up into the quadrupole units.

Here we calculate the energy associated with the interaction of these residual charges with the bulk that is made up of quadrupoles. For every such charge, we must integrate the charge-quadrupole interaction, where the integration is only on half a plane since the excess charges reside on the boundary.

The procedure is similar to the quadrupole-quadrupole calculation performed above, using complex coordinates. Let us calculate the charge-quadrupole interaction, assuming a positive charge at a distance z from the nearest charge in the quadrupole, also positive:

$$\begin{aligned} E^{cq}(z) = & \quad \Re\left(\ln(z) + \ln(z+1+i) + \ln(z+1) + \ln(z+i)\right) \\ = & \quad \Re\left(\ln\frac{i+1}{z} + \ln\frac{1}{z} + \ln\frac{i}{z}\right) \ . \end{aligned} \tag{A.7}$$

Allowing for a finite constant contribution from the near vicinity, we can expand for large z:

$$\begin{aligned} E^{cq}(z) \simeq & \quad \Re\left(\frac{i-1}{z^3}\right) \\ = & \quad \frac{\sin 3\Theta - \cos 3\Theta}{R^3} \ . \end{aligned} \tag{A.8}$$

This converges when integrated over the whole half plane. Hence each such charge contributes a finite correction to the energy and since there are $\sim \sqrt{N}$ such charges, the total contribution here grows with the size of the boundary.

Mutual interaction of single charges on the boundary

The residual charges also interact among themselves, an interaction we now calculate. Since the whole system is neutral and the bulk was defined as made neutral of quadrupoles then all excess charges on the boundary also have total zero charge. In all there are $M \sim \sqrt{N}$ such charges, so there are $\sim N$ pair interactions. Restricted to "checkerboard" placements they will typically be locally alternating in sign, or group up into multipoles.

Any charge-multipole interaction falls of fast enough (as can be seen in the previous calculations), so their total contribution to the energy will at most be a surface term.

We should mention that there are pathological cases where one charge type is concentrated on one side of the area with a typical spread of $r \sim \sqrt{N}$, distanced typically $R \sim \sqrt{N}$ from the opposite type ($r < R$) without violating the salt crystal lattice formation. Such a configuration will contribute a term that grows as $\sim N$ and violate the extensiveness. This contribution is positive, so constructing the crystal, at low temperature such that it relaxes to its preferable state will not create such configurations.

In all we managed to demonstrate that the total energy of a finite 2D salt crystal arrangement of charges is extensive with a lowest order surface correction term.

B Enumeration Details

We generated all SAWs for every quench studied so as to calculate the exact thermodynamic quantities. Actually, taking advantage of certain symmetries allowed us to generate less the the total number, thus reducing computation time.

There is a four-fold symmetry about the first step taken. This allows accounting only for walks that start, for example, in the positive x direction. There is another two-fold symmetry about the first step in the perpendicular direction, so we can consider only those that their first turn is in the positive y direction. The straight rod configuration does not have this last degeneracy, a fact that was taken into account.

In all, we were able to reduce the total number of configuration by a factor of almost $\frac{1}{8}$. Table 1 presents the actual number of SAWs generated for calculating a chain of N monomers.

N	*Configurations*
6	36
7	98
8	272
9	740
10	2,034
11	5,513
12	15,037
13	40,617
14	110,188
15	296,806
16	802,075
17	2,155,667
18	5,808,335
19	15,582,342
20	41,889,578
21	112,212,146
22	301,100,754
23	805,570,061
24	2,158,326,727
25	5,768,299,665
26	15,435,169,364

Table 1: Number of different SAWs enumerated for each length.

When enumerating all quenches, as for the configurations, certain symmetries allowed

generating only part of all the possible charge sequences.

A trivial symmetry was charge-conjugation of the whole sequence. The Hamiltonian is symmetric under negation of all charges. This allows the study of only the neutral and positively-charged quenches.

Because we generate all possible spatial configurations, there is also a start-end reversal symmetry. For every specific sequence and configuration, the reversed sequence will also have another configuration that results in the same state. This allows another reduction by a factor of almost $\frac{1}{2}$. Symmetric charge sequences do not have this degeneracy.

Table 2 presents the actual number of quenches generated for the lengths and excess charges, for which full enumeration was done.

N	*Excess Charge – Q*									
	0/1	2/3	4/5	6/7	8/9	10/11	12/13	14/15	16/17	18
6	10	9	3	1						
7	19	12	4	1						
8	38	28	16	4	1					
9	66	44	20	5	1					
10	126	110	60	25	5	1				
11	236	170	85	30	6	1				
12	472	396	255	110	36	6	1			
13	868	651	365	146	42	7	1			
14	1716	1519	1001	511	182	49	7	1		
15	3235	2520	1512	693	231	56	8	1		
16	6470	5720	4032	2184	924	280	64	8	1	
17	12910	9752	6216	3108	1204	344	72	9	1	
18	24310	21942	15912	9324	4284	1548	408	81	9	1

Table 2: Number of different quenches enumerated for each length fully enumerated (double headers refer to even/odd lengths).

References

[1] P. J. Flory, *Principles of Polymer Chemistry* (Cornell University Press, Ithaca, 1971).

[2] P. G. de Gennes, *Scaling Concepts in Polymer Physics* (Cornell University Press, Ithaca, 1979).

[3] A. Y. Grosberg and A. R. Khokhlov, *Statistical Physics of Macromolecules* (AIP Press, New York, 1994).

[4] H. Frauenfelder and P. G. Wolynes, Physics Today, Feb. 1994, 58.

[5] C. Tanford, *Physical Chemistry of Macromolecules* (John wiley & Sons, New York, 1967).

[6] E. Raphael and J. F. Joanny, Europhys. Lett. **13,** 623 (1990).

[7] H. S. Chan and K. A. Dill, Physics Today, Feb. 1993, 24.

[8] M. Kardar, Science **273,** 610 (1996); H. Li, R. Helling, C. Tang and N. Wingreen, Science **273,** 666 (1996).

[9] T. E. Creighton, *Proteins: Structures and Molecular Properties, 2nd Ed.* (W. H. Freeman and Company, New York, 1993).

[10] H. S. Chan and K. A. Dill, J. Chem. Phys. **95,** 3775 (1991).

[11] Y. Kantor and M. Kardar, Phys. Rev. E. **52,** 835 (1995).

[12] M. Plischke and B. Bergersen, *Equilibrium Statistical Physics, 2nd. Ed.* (World Scientific, Singapore, 1994).

[13] N. Madras and G. Slade, *The Self-Avoiding Walk*, (Birkhäuser, Boston, 1993).

[14] P. G. de Gennes, J. Phys. (Paris) Lett. **39,** L-55 (1975).

[15] Y. Kantor, M. Kardar and H. Li, Phys. Rev. E. **49,** 1383 (1994).

[16] S. F. Edwards, P. R. King and P. Pincus, Ferroelectrics, **30,** 3 (1980).

[17] P. G. Higgs and J. F. Joanny, J. Chem. Phys. **94,** 1543 (1991).

[18] S. K. Ma, *Statistical Mechanics* (World Scientific, Singapore, 1985).

[19] J.M. Victor and J. B. Imbert, Europhys. Lett. **24,** 189 (1993).

[20] J. Wittemer, A. Johner and J. F. Joanny, Europhys. Lett. **24,** 263 (1993).

[21] Y. Kantor, H. Li and M. Kardar, Phys. Rev. Lett. **69,** 61 (1992).

[22] Y. Kantor and M. Kardar, Phys. Rev. E. **51,** 1299 (1995).

[23] Y. Kantor and M. Kardar, Europhys. Lett. **27,** 643 (1994).

[24] A. M. Gutin and E. I. Shakhnovich, Phys. Rev. E. **50,** R3322 (1994).

[25] A. V. Dobrynin and M. Rubinstein, J. Phys. II France **5,** 677 (1995).

[26] Y. Levin and M. C. Barbosa, Euorophys. Lett. **31,** 513 (1995).

[27] B. Derrida, Phys. Rev. B. **24,** 2613 (1981).

[28] J. D. Bryngelson and P. G. Wolynes, Proc. Natl. Acad. Sci. USA **84,** 7524 (1987).

[29] E. Shakhnovich, G. Farztdinov, A .M. Gutin and M. Karplus, Phys. Rev. Lett. **67,** 1665 (1991).

[30] E. Shakhnovich, A. Gutin, J. Chem. Phys. **93,** 5967 (1990).

[31] E. Shakhnovich, A. M. Gutin, J. Phys. A. **22,** 1647 (1989).

[32] E. Shakhnovich, A. M. Gutin, Biophys. Chem. **34,** 187 (1989).

[33] A. Dinner, A. Sali, M. Karplus and E. Shakhnovich, J. Chem. Phys. **101,** 1444 (1994).

[34] V. S. Pande, A. Y. Grosberg, C. Joerg and T. Tanaka, Phys. Rev. Lett. **76,** 3987 (1996).

[35] V. S. Pande, A. Y. Grosberg, C. Joerg, M. Kardar and T. Tanaka, Phys. Rev. Lett. **77,** 3565 (1996).

[36] M. E. Fisher, J. Stat. Phys. **75,** 1 (1994).

[37] Y. Levin, X. Li and M. E. Fisher, Phys. Rev. Lett. **73,** 2716 (2716).

[38] J. M. Kosterlitz and D. J. Thouless, J. Phys. C. **6,** 1181 (1973).

[39] P. Minnhagen, Rev. Mod. Phys. **59,** 1001 (1987).

[40] C. Deutsch and M. Lavaud, Phys. Rev. A. **9,** 2598 (1974).

[41] J. M. Caillol and D. Levesque, Phys. Rev. B. **33,** 499 (1986).

[42] M. E. Fisher, X. Li and Y. Levin, J. Stat. Phys. **79,** 1 (1995).

[43] J. R. Lee and S. Teitel, Phys. Rev. B. **46,** 3247 (1992).

[44] I. Golding and Y. Kantor, cond-mat/9704244 (1997).

[45] M. R. Ejtehadi and S. Rouhani, cond-mat/9606077 (1996).

[46] R. L. Pathria, *Statistical Mechanics* (Pergamon Press, Oxford, 1972).

[47] M. Abramowitz and I. A. Stegun, *Handbook of Mathematical Functions* (Dover Publications, New York, 1965).

[48] M. E. Fisher and D. Ruelle, J. Math. Phys. **7,** 260 (1966).

TEL AVIV UNIVERSITY
RAYMOND AND BEVERLY SACKLER
FACULTY OF EXACT SCIENCES
SCHOOL OF PHYSICS & ASTRONOMY

אוניברסיטת תל-אביב
הפקולטה למדעים מדוייקים
ע"ש ריימונד ובברלי סאקלר
בית הספר לפיסיקה ואסטרונומיה

פולימרים דו-מימדיים עם אינטראקציות קולון אקראיות

חיבור זה מוגש כחלק מן הדרישות לקבלת תואר "מוסמך למדעים" M.Sc.

בית הספר לפיסיקה ואסטרונומיה

אוניברסיטת תל–אביב

על–ידי

אילון ברנר

העבודה הוכנה בהדרכתו של פרופסור יעקב קנטור

יוני 1997